JOURNAL OF RESEARCH of the National Bureau of Standards—D. Radio Propagation
Vol. 66D, No. 4, July–August 1962

Representation of Diurnal and Geographic Variations of Ionospheric Data by Numerical Methods*

William B. Jones and Roger M. Gallet

Contribution from Central Radio Propagation Laboratory, National Bureau of Standards, Boulder, Colo.

(Received February 15, 1962)

A solution is given to the problem of representing the complex properties of ionospheric characteristics on a worldwide scale, including their diurnal variation, by numerical analysis of ionospheric data as they are obtained from a network of sounding stations, without prior hand operations. The problem is complicated by two basic difficulties: (1) the data are affected by noise (random fluctuation) and (2) the stations are irregularly positioned in the two space dimensions. The second difficulty is overcome by a general method for constructing functions orthogonal relative to the distribution of the stations. Special filtering processes are employed for the optimum separation of noise from real physical variations. The end product of the analysis is a table of numerical coefficients defining a function Γ (λ, θ, t) of three variables, latitude (λ), longitude (θ) and time (t), which can be used to compute the ionospheric characteristic at any desired location or instant of time. The method applies to any ionospheric characteristic; however, as a means of illustration we use in the present paper only the characteristic, monthly median of the $F2$-layer critical frequency (f_0F_2).

1. Introduction

It is well known that the ionosphere experiences diurnal and geographic variations, as well as long term variations connected with seasons and the 11 year solar cycle. Although many of these variations are systematic and predictable with a considerable degree of accuracy, for the F-layer theoretical models do not yet give good representation of many of the details. Therefore, worldwide representations of F-layer characteristics are best made using measurements obtained from a network of sounding stations.

Ionospheric maps have been made and still are being produced by persons having considerable knowledge of ionospheric data and experience in drawing maps. Many graphic techniques are employed for smoothing raw data and for eliminating inconsistencies. However, such procedures are relatively slow and tedious and, to some extent, are not repeatable. The accuracy, as well as repeatability, are dependent upon the skill, knowledge, and experience of the people carrying out the subjective steps of the process. Moreover, as a means of simplifying hand operations, unrealistic assumptions have been made, such as the "longitude zone system," in which no longitudinal variation is taken into account or represented within the defined longitude zones.

Several years ago, the authors attacked the problem of representing the complex properties of ionospheric characteristics on a worldwide scale, including their diurnal variation, by numerical analysis of ionospheric data as they are measured at the stations, without prior hand operations.[1] The problem is complicated by two basic difficulties: (1) the data are affected by noise—random fluctuations produced from a number of sources (ch. 4)—and (2) the ionospheric stations (fig. 1) are irregularly positioned on the earth. The *noise* would produce a very rough and physically unacceptable map if the original data were represented exactly without time and space smoothing. Thus a certain amount of smoothing is necessary, but too much smoothing would give a map which does not respect the true physical variation as well as possible. The *irregular distribution of stations* presents problems both in data-fitting (ch. 2) and in preserving the stability and physical soundness of the representation in areas where few if any stations are available (ch. 5). Also the fact that the set of available stations varies from month to month complicates the data-fitting processes and the comparison of numerical representations for different months. In the past, people experienced in drawing maps have overcome these difficulties more or less intuitively using empirical knowledge of the ionosphere and good sense. It is not easy to give these qualities to a computing machine.

The solution[2] to the problem consists of well-defined mathematical operations—described and illustrated in the present paper—which have been programed for use on several large-scale digital computers.[3] Input to the computer program consists of the measurements of an ionospheric characteristic from all available stations for a given month. The diurnal variation is represented by Fourier analysis of the 24 hourly measurements from each available

* A sequel paper on "Methods for applying numerical maps of ionospheric characteristics" will appear in an early issue of this journal.

[1] The need for mapping methods based on numerical methods and the use of high-speed computers has been felt for several years [CCIR, 1959].

[2] For a brief summary the reader can refer to [Jones and Gallet, 1960].

[3] The computer program has been developed completely for both the IBM 704 and 7090 computers and in part for the CDC 1604.

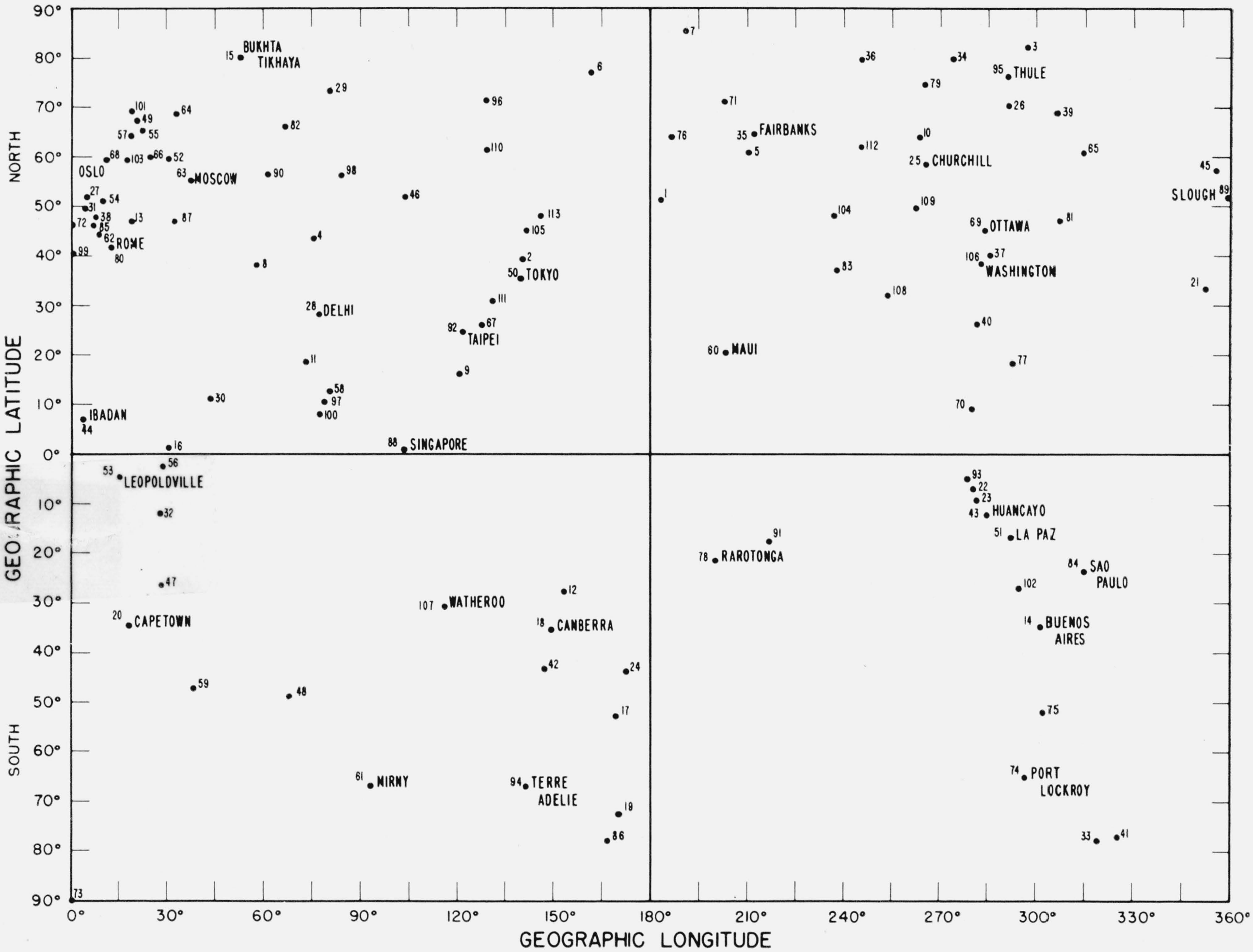

Figure 1. *Map of ionospheric stations for December 1957.*

station (sec. 3.1). Then the worldwide geographic variation of each Fourier coefficient is expanded in a series of functions analogous to surface spherical harmonics (sec. 3.3). The optimum separation of noise is obtained by truncation of orthonormal series (ch. 4). At the end of the analysis the diurnal and geographic variations of the characteristic are represented by a relatively small table of coefficients defining a function of three variables: latitude, longitude, and time of day. Such a function is referred to as a "numerical map" (ch. 7).

The methods used here are general enough to be applied to any ionospheric characteristic. In fact, they have already been successfully used to represent such characteristics as: the critical frequency (f_oF_2), the 3,000 km maximum usable frequency factor ($F2$–M3000), the maximum electron density (N-max), the height of N-max, and the quarter thickness of a layer. With only slight modification the methods can also include variations with height above the surface of the earth. For the sake of illustration, we restrict ourselves here to the characteristic f_oF_2 monthly median, since this characteristic is the most important one for radio propagation, and its variations are the most difficult to represent. In chs. 2 and 6, we outline briefly the mathematical methods employed in this analysis.

2. General Data Fitting Method

As was mentioned in the introduction, the geographic variation of each Fourier coefficient (obtained from the diurnal analysis) is represented by series of functions analogous to surface spherical harmonics. The approach generally used in global analyses of geophysical data has been to first draw contour maps by hand and then to analyze in spherical harmonics the values read from the maps at the intersections of a regular grid. However, such methods incorporate many of the undesirable features of the hand operations used currently to produce ionospheric maps (ch. 1).

We have attacked this problem from the opposite direction by first analyzing the data directly as they are obtained from the stations. Then contour maps are computed *from the analyses* when desired.[4]

[4] Examples of such contour maps are shown in figures 11a, 11b, 12, and 13.

The method used is mathematically well defined, entirely repeatable, well adapted to automatic computing and, in a sense, more objective than the hand methods previously mentioned. As a result of this new approach, we have had to face some additional complications (ch. 5). In the expansion of the geographic variation it is natural to use orthogonal [5] functions, since an optimum cutoff of the series has to be made (ch. 4). The classical spherical harmonic functions [Byerly, 1893, pp. 144–218] could not be used, however, since they are not orthogonal relative to the positions of stations. Thus we have had to construct functions—analogous to spherical harmonics (sec. 3.3)—which are orthogonal with respect to the irregularly spaced coordinates of the stations. The problem is even more complicated by the fact that the set of available stations varies from month to month, making it necessary to construct new orthogonal functions for the analysis of each month's data.

For this purpose we have employed the very general data-fitting method described briefly in this chapter. Of course, the method also applies to the Fourier analysis of the equally spaced measurements of the diurnal variation. In the following discussion, the points x_i (where the measurements are made) can be any set

$$x_i=(x_{i1}, x_{i2}, \ldots, x_{iM}) \qquad i=1, 2, \ldots, N$$

irregularly positioned in an M dimensional space. The coordinate functions $G_k(x)$, which are fitted to the data by the method of least squares, can be any linearly independent functions of M variables (e.g., elementary transcendental functions, Chebychev polynomials, or spherical harmonics).

2.1. Least Squares Method

Let $y_1, y_2, \ldots, y_N$ denote measurements of an ionospheric characteristic taken at the points $x_1, x_2, \ldots, x_N$. Suppose that a *class of functions* $Y_\alpha(x)$ is given and a *criterion* for evaluating how well each of these functions fits the values y_i. (We will take $Y_\alpha(x)$ as linear sums of coordinate functions $G_k(x)$.) Then the problem of data-fitting is to determine that function $Y(x)$ from the given class which "best" fits the y_i relative to the given criterion. We have chosen the *least squares* criterion since it is well-adapted to the analysis of data affected by noise and it is far easier to compute than other methods such as the minimax [Stiefel, 1959]. The question of choosing the proper classes of functions $Y_\alpha(x)$ is discussed in chapter 3.

We assume given a set of linearly independent coordinate functions, $G_0(x), G_1(x), \ldots, G_K(x)$, with $K<N$, and it is required by the least squares criterion to find that function

$$Y_K(x)=\sum_{k=0}^{K} D_k G_k(x) \tag{1}$$

for which the sum of squares of residuals

$$E_K=\sum_{i=1}^{N} [y_i-Y_K(x_i)]^2 \tag{2}$$

has a minimum value with respect to all real coefficients D_k.[6] It is easily shown that necessary and sufficient conditions for E_K to be minimized are

$$\frac{\partial E_K}{\partial D_k}=0, \qquad k=0, 1, \ldots, K. \tag{3}$$

These give the well known *normal equations*

$$\sum_{k=0}^{K} D_k(G_m,G_k)=(y,G_m), \qquad m=0, 1, \ldots, K \tag{4}$$

where we adopt the notation

$$(G_m,G_k)=\sum_{i=1}^{N} G_m(x_i)G_k(x_i),$$

and

$$(y,G_m)=\sum_{i=1}^{N} y_i G_m(x_i), \tag{5}$$

and we will later use

$$(y,y)=\sum_{i=1}^{N} y_i^2.$$

For solving the normal equations (and for a number of other reasons to be discussed) we have made extensive use of orthogonal functions.

2.2. Gram-Schmidt Orthogonalization

A set of functions $A_0(x), A_1(x), \ldots, A_K(x)$ is said to be *orthogonal* with respect to the points $x_1, x_2, \ldots, x_N$, if

$$(A_k,A_m)=0 \qquad \text{when } k\neq m. \tag{6}$$

Thus we see that if the coordinate functions $G_k(x)$ were orthogonal, the system of normal eq (4) would be *uncoupled* and its solution would be simply

$$D_k=\frac{(y,G_k)}{(G_k,G_k)}, \qquad k=0, 1, \ldots, K. \tag{7}$$

On the other hand, we can apply the Gram-Schmidt orthogonalization process [Davis and Rabinowitz, 1954] [7] to form the system of functions

$$A_0(x)=G_0(x) \tag{8}$$

$$A_k(x)=\sum_{p=0}^{k-1} a_{kp}A_p(x)+G_k(x), \qquad k=1, 2, \ldots, K,$$

[5] The term "orthogonal" is used here in the sense of a discrete distribution [Szegö, 1959, pp. 33–37].

[6] For simplicity we have written D_k with only one subscript k. However, we must remember that the terms in (1) are generally not independent and therefore all of the coefficients depend on the value of K.

[7] Our procedure differs from that of Davis and Rabinowitz [1954] in that we have reversed the order of orthogonalization and normalization in order to reduce the accumulative rounding error. (See sec. 2.3 and also ch. 6.)

satisfying (6), where the coefficients a_{kp} are given by

$$a_{kp}=-\frac{(G_k,A_p)}{(A_p,A_p)}. \tag{9}$$

Then the least squares solution $Y_K(x)$ can be written in the form

$$Y_k(x)=\sum_{k=0}^{K} a_k A_k(x) \tag{10}$$

where

$$a_k=\frac{(y,A_k)}{(A_k,A_k)}, \qquad k=0,1, \ldots, K. \tag{11}$$

The orthogonal series (10) is, of course, sufficient for many purposes, but in our applications it is useful to have $Y_K(x)$ in the simpler form (1). For this purpose we compute the triangular matrix

$$\begin{array}{cccccccc} l_{00} & l_{01} & l_{02} & \cdot & \cdot & \cdot & l_{0,K-2} & l_{0,K-1} & l_{0,K} \\ l_{10} & l_{11} & l_{12} & \cdot & \cdot & \cdot & l_{1,K-2} & l_{1,K-1} & \\ \cdot & \cdot & \cdot & \cdot & \cdot & \cdot & \cdot & \cdot & \\ \cdot & \cdot & \cdot & \cdot & \cdot & \cdot & \cdot & & \\ l_{K-1,0} & l_{K-1,1} & & & & & & & \\ l_{K,0} & & & & & & & & \end{array} \tag{12}$$

where the elements l_{pk} are obtained by

$$\begin{aligned} &l_{0k}=a_k && 0\leqq k\leqq K \\ &l_{pk}=l_{p-1,k}+l_{p-1,K-(p-1)}a_{K-(p-1),k} && 1\leqq p\leqq K \\ & && 0\leqq k\leqq K-p \end{aligned} \tag{13}$$

starting with the top row and going from left to right. Then we have for the desired coefficients

$$D_k=l_{K-k,k}. \tag{14}$$

A number of advantages are gained from the use of orthogonal functions. As was previously shown the $A_k(x)$ *uncouple* the system of normal equations so that terms in the series (10) are *independent*. As a consequence we obtain automatically the least squares solution $Y_k(x)$ for all degrees from zero through K, and therefore can test the physical significance of each term to determine where the series should be truncated (ch. 4). Moreover, the computation of E_K is greatly facilitated since by substituting (10) into (2) and applying (6) and (11), we obtain

$$E_K=(y,y)-\sum_{k=0}^{K} a_k^2(A_k,A_k). \tag{15}$$

Hence E_k is computed recursively for each degree by

$$E_0=(y,y)-a_0^2(A_0,A_0) \tag{16}$$

$$E_k=E_{k-1}-a_k^2(A_k,A_k) \qquad \text{for} \qquad 1\leqq k\leqq K.$$

It should also be mentioned that in the construction of the orthogonal functions $A_k(x)$ we use only the set of points x_i and the functions $G_k(x)$. Consequently when several different sets of values y_i are measured at the same set of points x_i and are to be fitted by sums of the same functions $G_k(x)$, only one orthogonal system is required to uncouple all of the resulting systems of normal equations. Thus in the representation of geographic variations of Fourier coefficients, the same set of orthogonal functions can be used for all Fourier coefficients for a given month. This is an important factor in the economization of computer time, since—as will be shown in chapter 4—there are 17 Fourier coefficients to be represented in the analysis of f_0F_2.

2.3. Normalization

A set of functions $F_1(x), F_2(x), \ldots, F_K(x)$ is said to be *orthonormal* with respect to the points $x_1, x_2, \ldots, x_N$ if, in addition to the orthogonality conditions (6), they also satisfy

$$(F_k,F_k)=1 \qquad \text{for } k=0, 1, \ldots, K. \tag{17}$$

When $Y_K(x)$ is expressed in the form

$$Y_K(x)=\sum_{k=0}^{K} d_k F_k(x), \tag{18}$$

the *orthonormal coefficients* d_k have the simplified formula

$$d_k=(y,F_k) \qquad k=0, 1, \ldots, K \tag{19}$$

and

$$E_k=E_{k-1}-d_k^2, \qquad 1\leqq k\leqq K. \tag{20}$$

One main advantage of this normalization is that the significance of each term $d_kF_k(x)$ in (18)—determined by the reduction it makes on the sum of squares of residuals (20)—is seen in the relative size of d_k^2. Another advantage is obtained from the simplified interpretation of these functions as *unit* (orthogonal) *vectors* in an N dimensional vector space (ch. 6).

Using the relation

$$F_k(x)=\frac{A_k(x)}{\sqrt{(A_k,A_k)}} \tag{21}$$

and (8), the generation of the orthonormal functions $F_k(x)$ becomes

$$F_k(x)=\sum_{p=0}^{k-1} d_{kp}F_p(x)+d_{kk}G_k(x) \tag{22}$$

where

$$d_{kp}=a_{kp}\sqrt{\frac{(A_p,A_p)}{(A_k,A_k)}} \qquad 0\leqq p\leqq k-1$$

and

$$d_{kk}=\frac{1}{\sqrt{(A_k,A_k)}}. \tag{23}$$

Then from (19), (22), and (11), the coefficients in the solution (18) become

$$d_k = a_k\sqrt{(A_k, A_k)}. \tag{24}$$

The application of the Gram-Schmidt orthogonalization process to least squares problems has been treated in a paper by Davis and Rabinowitz [1954]. For completeness we included here an outline of their development with one modification—the order of orthogonalization and normalization is reversed. The advantage of this modification is that accumulative rounding error can be considerably reduced. Whereas we compute (A_k, A_k) as a sum of squares, the procedure in the reference cited above is to compute it as a difference of positive numbers

$$(A_k, A_k) = (G_k, G_k) - \sum_{p=0}^{k-1} (G_k, F_p)^2,$$

which can be so small as to result in total loss of significant digits. As can be seen from (23), errors in (A_k, A_k) have a strong *accumulative* effect on the construction of the functions $F_k(x)$.

We have also found, however, that a very serious additional rounding error [8] accumulates in the Gram-Schmidt orthogonalization process when the coordinate functions $G_k(x)$ are far from being orthogonal. That such rounding errors can have a significant effect on the least squares solution is shown in chapter 6 by a numerical example with errors occurring by as much as 30 percent. It is well known that similar types of errors occur when solving the normal eq (4) by other methods.[9] Thus the danger of accumulative rounding error is not so much a characteristic of the particular method we have used, but is an inherent difficulty in all large-scale least squares problems. Also included in chapter 6 are an explanation of the process of accumulation of the error, a quantitative method for estimating its effect, and a *reorthogonalization* process which keeps the rounding error under control no matter how large the system.

For the diurnal representation of the data, we use Fourier series which are particular orthonormal series for equally-spaced data points. For the geographic variation we employ an orthonormal series constructed from the procedures described above.

3. Choice of Functions

3.1. Diurnal Variation

The most natural method for representing the diurnal variation is Fourier analysis, since ionospheric characteristics are periodic functions of time. Moreover, the trigonometric functions associated with Fourier analysis are automatically orthogonal with respect to the equally-spaced points of measurement; hence the computational problems of least squares fitting are greatly simplified. Since the observations are made at each hour in the zone time (ZT) of each station, they cannot be intercompared for different stations until time corrections are made. As will be shown, Fourier analysis provides a simple means for such corrections. The most important use of Fourier analysis, however, is in the separation of "noise" (random error) from the "real" diurnal variation of the data (ch. 4).

We give here the essential formulas employed; for more comprehensive treatment, the reader can refer to numerous texts on Fourier analysis. Let x denote the *zone time hour angle* (degrees) defined by

$$x = 15^\circ\ (\mathrm{ZT}) - 180^\circ, \tag{25}$$

where ZT is given in hours. Thus, for example $x=0^\circ$ at noon (ZT). We let $y_1, y_2, \ldots, y_{24}$ denote the hourly measurements corresponding to the hours

$$x_i = 15^\circ i \qquad i=1, 2, \ldots, 24, \tag{26}$$

respectively, and we choose 1, $\cos jx$ and $\sin jx$ ($j=1, 2, \ldots, H$, and $2H+1 \leqq 24$) as coordinate functions $G_k(x)$. It is well known that these functions are orthogonal with respect to the points (26). Therefore from (7) the least squares solution has the form

$$Y_{2H+1}(x) = \alpha_0 + \sum_{j=1}^{H} [\alpha_j \cos jx + \beta_j \sin jx], \tag{27}$$

where

$$\begin{aligned} \alpha_0 &= \frac{1}{24}\sum_{i=1}^{24} y_i \\ \alpha_j &= \frac{1}{12}\sum_{i=1}^{24} y_i \cos jx_i, \qquad\qquad 1 \leqq j \leqq H. \\ \beta_j &= \frac{1}{12}\sum_{i=1}^{24} y_i \sin jx_i \end{aligned} \tag{28}$$

Equation (27) can also be written in the convenient form

$$Y_{2H+1}(x) = \alpha_0 + \sum_{j=1}^{H} c_j \cos (jx - \phi_j) \tag{29}$$

where the *amplitude* c_j and *phase* ϕ_j are given by

$$c_j = \sqrt{a_j^2 + b_j^2} \quad \text{and} \quad \phi_j = \arctan \frac{\beta_j}{\alpha_j}. \tag{30}$$

Corrections to Local Mean Time

In order to intercompare data from different stations it is necessary to correct for the small difference between the actual *local mean time* (LMT) at each station and the time at the reference longitude θ_R of the zone. Such corrections can be made very simply in (29) by a shift of the phase where

$$\psi_j = \phi_j + j(\theta - \theta_R), \tag{31}$$

θ is the longitude (degrees east of Greenwich) of the station. Therefore the *representation of the diurnal variation* takes the form

[8] The process of accumulation of rounding error is similar to that described by Lanczos [1956, pp. 123–130].

[9] See for example [Lanczos, 1956, pp. 118–122; Kunz, 1957; Forsythe, 1957, p. ;77 Forsythe and Rosenbloom, 1958, pp. 20–21, and references contained therein].

$$U_{2H+1}(t) = a_0 + \sum_{j=1}^{H} [a_j \cos jt + b_j \sin jt] \qquad (32)$$

where the Fourier coefficients *corrected to LMT* are given by

$$a_0 = \alpha_0$$

$$a_j = c_j \cos \psi_j \qquad b_j = c_j \sin \psi_j, \qquad (33)$$

and t denotes the local mean hour angle,

$$t = 15° (\text{LMT}) - 180°.$$

3.2. Main Latitudinal Trend

The Fourier coefficients are corrected to LMT (sec. 3.1) so that their main geographic variation becomes latitudinal and is therefore greatly simplified.[10] Among the first problems to be solved for representing this variation was that of selecting a suitable set of coordinate functions $G_k(x)$ for the least squares fit. Polynomials seemed to be the most natural type of function, but the question arose as to what would be the best independent variable for the polynomials. The simplest variable tried was the *geographic latitude* λ. However, when a sufficiently high degree was taken, the polynomials in λ became unstable (i.e., wildly fluctuating) in regions such as near the poles where little or no data were available (figs. 2 and 3). Much more stable representations were obtained by using polynomials in $\sin \lambda$. Moreover, it was found that the equatorial variation could be represented in more detail by these functions than by the polynomials in λ of the same degrees (figs. 2 and 3).

[10] An atlas of graphs of the geographic variations of the Fourier coefficients for f_0F_2 median for four seasonal months has been prepared and will soon appear as an NBS Technical Note [Jones, 1962]. This atlas illustrates the very systematic and well-defined variations of these coefficients.

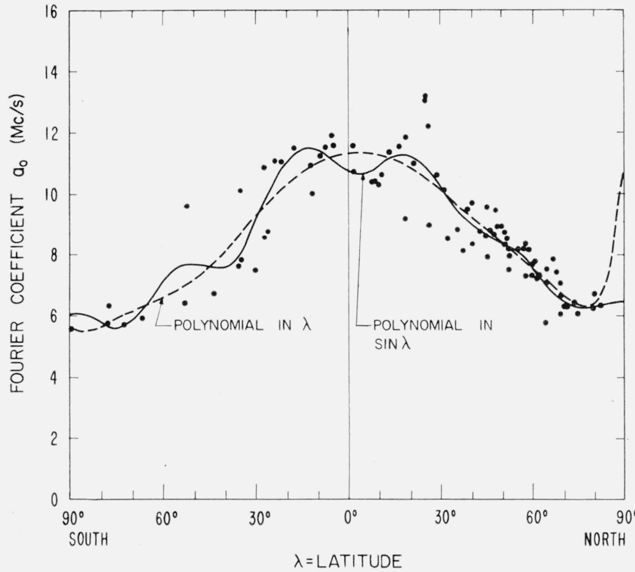

FIGURE 2. *Representation of main latitudinal variation of Fourier (time series) coefficients* a_0 *for* f_0F_2 *monthly median by least squares polynomials of degree 10.*

December 1957 96 stations.

One explanation of the superiority of the variable $\sin \lambda$ is the following. The fitting of polynomials in $\sin \lambda$ to data located at a set of latitudes λ_i is equivalent to fitting polynomials in a variable x to the same data located at the correspondingly shifted set of points $x_i = \sin \lambda_i$. The shifting of the data resulting from this transformation has the effect of pulling the data symmetrically away from the equator toward the poles. Thus the data become more uniformly distributed in the interval $-1 \leqq x \leqq 1$, and the sharpness of the variation near the equator is reduced. To illustrate this spreading effect the same data shown in figures 2 and 3 have been plotted against $\sin \lambda$ in figure 4, together with the polynomial of degree 10 in $x = \sin \lambda$.

A second explanation of the improved behavior of the polynomials in $x = \sin \lambda$ can be given in terms of the corresponding orthonormal functions. Choosing powers of the independent variable as coordinate functions, we generate (secs. 2.3 and 2.4) one orthonormal system $F_k^{(1)}(\lambda)$ corresponding to the station latitudes λ_i and a different system $F_k^{(2)}(\sin \lambda)$ corresponding to the shifted set of points $x_i = \sin \lambda_i$. The resulting least squares representations take the forms

$$Y_{k_0}^{(1)}(\lambda) = \sum_{k=0}^{k_0} d_k^{(1)} F_k^{(1)}(\lambda),$$

$$Y_{k_0}^{(2)}(\sin \lambda) = \sum_{k=0}^{k_0} d_k^{(2)} F_k^{(2)}(\sin \lambda), \qquad (34)$$

respectively. A comparison of the different orthonormal functions (for degrees 8 to 10) is shown in figure 5. To simplify the comparison, an additional normalization was made so that all of the graphs have a common value at the right end point. It can

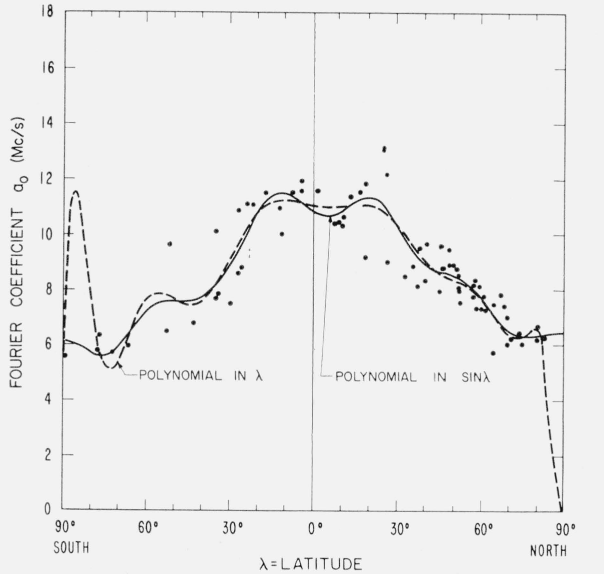

FIGURE 3. *Representation of main latitudinal variation of Fourier (time series) coefficients* a_0 *for* f_0F_2 *monthly median by least squares polynomials of degree 13.*

December 1957 96 stations.

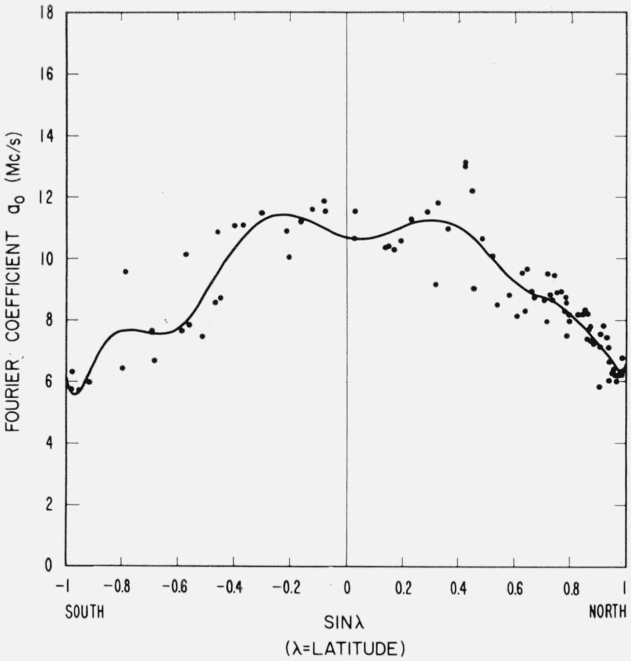

FIGURE 4. *Representation of main latitudinal variation of Fourier (time series) coefficients* a_0 *for* f_0F_2 *monthly median by least squares polynomial (degree 10) in sin* λ.

December 1957 96 stations.

be seen that at high degree ($8 \leq k \leq 10$) the polynomials in λ have very large values near the right end point compared with their values near the center. Thus to represent the strong geographic variation near the equator the polynomials $F_k^{(1)}(\lambda)$ of high degree have to be multiplied by large coefficients $d_k^{(1)}$, which results in the blowing up effect near the poles (figs. 2 and 3). In contrast, for the polynomials $F_k^{(2)}(\sin\lambda)$ the maximum amplitude of oscillation is more uniform throughout the interval, hence the greater stability of $Y_{k_0}^{(2)}(\sin\lambda)$ near the poles. In addition we see that near the center of the interval the distances between successive maxima and minima are less for the $F_k^{(2)}(\sin\lambda)$ than for the $F_k^{(1)}(\lambda)$. Thus we can understand the better representation of equatorial variation by $Y_{k_0}^{(2)}(\sin\lambda)$.

To conclude this discussion we note that the behavior of the polynomials $F_k^{(1)}(\lambda)$ resembles that of the classical *Legendre polynomials* [Byerly, 1893, pp. 184–185]. On the other hand, the amplitude distribution of the $F_k^{(2)}(\sin\lambda)$ more nearly approximates the exactly uniform distribution of the classical *Chebychev polynomials* [Jones, Miller, Conn, and Pankhurst, 1946, pp. 194–195]. It is well known that orthogonal series of Legendre polynomials tend to blow up near the end points [Lanczos, 1938, pp. 144–145], whereas series of Chebychev polynomials minimize the maximum error, and therefore are as

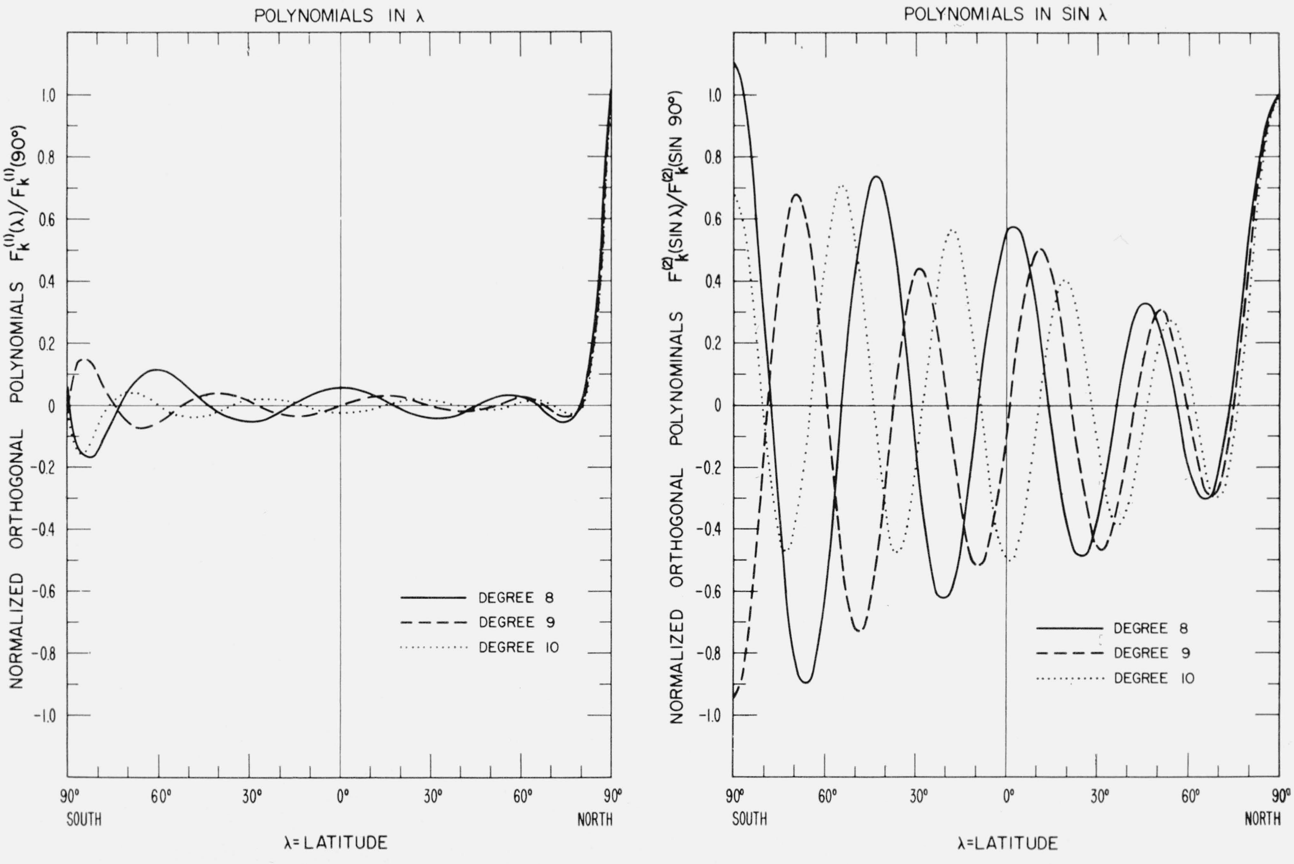

FIGURE 5. *Orthogonal polynomials defined by ionospheric station latitudes.*

December, 1957——96 stations.

stable at the end points as they are at the center. Thus by analogy one would expect the behavior demonstrated in figures 2 and 3.

A similar study was also made with polynomials in the variable sin [90° sin λ], which is the natural extension of the spreading process described above. In this case, the representation was improved even more around the equator, but significant geographic variation in the temperate latitudes was squeezed into the poles and so lost. Therefore polynomials in sin λ were chosen for representing the main latitudinal trend. The determination of the "best degree" for these polynomials is discussed in chapters 4 and 5.

3.3. Mixed Latitudinal and Longitudinal Variations

The existence of systematic longitudinal variation[11] is illustrated by the graph in figure 6 of Fourier (time series) coefficients a_1—first harmonic, cosine part—for f_0F_2 monthly median, plotted against latitude λ. Also shown in the figure is the representation of the main latitudinal trend by means of a polynomial of degree 10 in sin λ. By means of special plotting symbols used to signify approximate station longitudes (see legend), we see that the coefficients are not randomly dispersed about the main latitudinal trend, but—in certain regions, particularly around the equator—are systematically arranged according to *longitude* θ. We

[11] That the longitudinal variation, illustrated in figure 6, is consistent for different seasons and for periods of high and low solar activity is demonstrated by the atlas of graphs of Fourier coefficients for f_0F_2 monthly median referred to at the beginning of section 3.2.

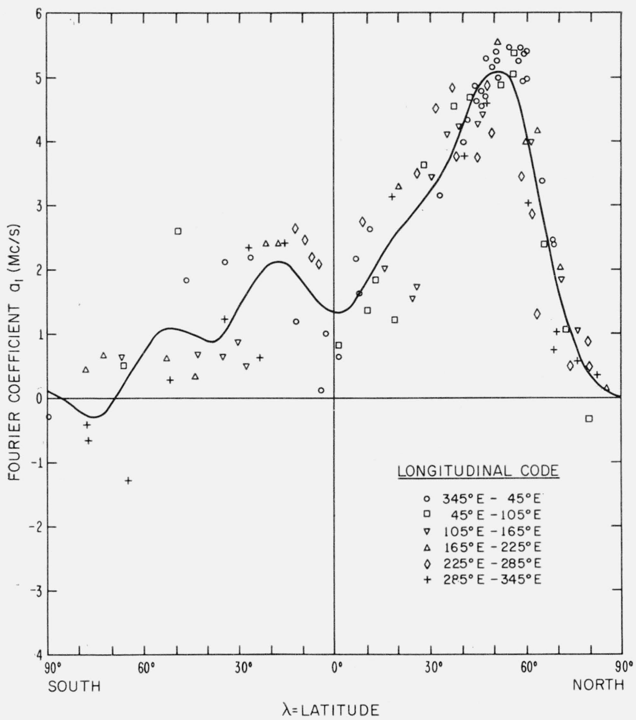

FIGURE 6. *Representation of main latitudinal variation of Fourier (time series) coefficients a_1 for f_0F_2 monthly median by least squares polynomial (degree 10) in sin λ.*

December 1957 113 stations.

discuss here the choice of functions for representing these second order mixed latitudinal and longitudinal variations.

The usual method of representing global variations of geophysical phenomena is by spherical harmonic analysis [Byerly, 1893, pp. 144–218]. However, the classical surface spherical harmonics—satisfying LaPlace's equation—are not orthogonal with respect to the positions (λ_i,θ_i) of the ionospheric stations. Therefore for convenience, and with no loss of generality, we choose as our coordinate functions the simplest set $G_k(\lambda,\theta)$ (see table 1) of which the surface spherical harmonics are linear combinations. A particular set of the functions G_k can be specified by assigning the values q_0, q_1, and q_2 which are, respectively, the highest powers of sin λ for terms involving: (1) no longitudinal variation, (2) first order longitudinal variation, and (3) second order longitudinal variation. Equivalently, we could also specify the values k_0, k_1, and $k_2=K$ taken by the index k at the end of each of the three groups of the $G_k(\lambda,\theta)$. These values are related to the q-values by the equations

$$k_0=q_0 \qquad k_r=k_{r-1}+2(q_r+1) \text{ for } r=1, 2. \quad (35)$$

From table 1 we see that the first group of functions (powers of sin λ) is the same set chosen (sec. 3.2) for the main latitudinal trend. We note that the zonal harmonics are linear combinations of these functions, and the first and second order sectorial and tesseral harmonics are linear combinations of the first and second order terms in longitude (see table 1) used for the mixed latitudinal and longitudinal variation. As a consequence, a least squares representation in the form of a linear combination of the $G_k(\lambda,\theta)$ has many properties of a spherical harmonic analysis. For example, it is periodic in longitude and constant at the poles, and the first and second order terms in longitude are weighted according to latitude by the functions cos λ and $\cos^2$ λ, respectively. In fact, a series in the $G_k(\lambda,\theta)$ is identical—but expressed in a different form—to that which would be obtained from spherical harmonic analysis.

TABLE 1. *Geographic functions* $G_k(\lambda,\theta)$

Main latitudinal variation		Mixed latitudinal and longitudinal variation			
		First order in longitude		Second order in longitude	
k	$G_k(\lambda,\theta)$	k	$G_k(\lambda,\theta)$	k	$G_k(\lambda,\theta)$
0	1	k_0+1	$\cos\lambda\cos\theta$	k_1+1	$\cos^2\lambda\cos 2\theta$
1	$\sin\lambda$	k_0+2	$\cos\lambda\sin\theta$	k_1+2	$\cos^2\lambda\sin 2\theta$
2	$\sin^2\lambda$	k_0+3	$\sin\lambda\cos\lambda\cos\theta$	k_1+3	$\sin\lambda\cos^2\lambda\cos 2\theta$
		k_0+4	$\sin\lambda\cos\lambda\sin\theta$	k_1+4	$\sin\lambda\cos^2\lambda\sin 2\theta$
k_0	$\sin^{q_0}\lambda$				
		k_1-1	$\sin^{q_1}\lambda\cos\lambda\cos\theta$	$K-1$	$\sin^{q_2}\lambda\cos^2\lambda\cos 2\theta$
		k_1	$\sin^{q_1}\lambda\cos\lambda\sin\theta$	K	$\sin^{q_2}\lambda\cos^2\lambda\sin 2\theta$

The geographic variation of a Fourier (time series) coefficient is therefore represented by a function of the form

$$Y_K(\lambda,\theta)=\sum_{k=0}^{K} d_k F_k(\lambda,\theta)=\sum_{k=0}^{K} D_k G_k(\lambda,\theta) \tag{36}$$

where the $F_k(\lambda,\theta)$ are orthonormal functions defined with respect to the positions of the ionospheric stations (taking as coordinate functions the $G_k(\lambda,\theta)$ in table 1), and the coefficients d_k and D_k are obtained by the method of least squares (ch. 2). The determination of the "best" representation with these functions is discussed in chapters 4 and 5.

4. Optimum Separation of Noise From Real Physical Variation

It was previously mentioned that ionospheric data are affected by noise (random fluctuation) produced from a number of sources. The noise is due in part to limitations of equipment at various stations and to errors of scaling and rounding. A large part of the noise is the result of statistical fluctuations in the sample medians, the sample size being at most 31 and frequently much less. These fluctuations are, to some degree, caused by intrinsic variation of the physical phenomena being measured.

The noise is evidenced by such occurrences as unusual roughness or unrealistic flattening of the diurnal plots during certain hours. The presence of noise is also suggested by random inconsistencies of data at groups of neighboring stations as observed from data-comparisons on a worldwide basis. In the present chapter, however, we give more *objective evidence* of the noise by means of statistical and mathematical data-analyses. Included are methods for quantitative estimation of the noise and for its optimum separation from real physical variation.

We shall therefore consider ionospheric data as sampled values y_i from a function $f(x)$ which is the sum of two components: (1) the real physical characteristic $f_1(x)$, and (2) a random noise component $f_2(x)$. Thus we consider each value y_i as a sum

$$y_i=y_i^{(1)}+y_i^{(2)} \tag{37}$$

where

$$y_i^{(1)}=f_1(x_i) \text{ and } y_i^{(2)}=f_2(x_i). \tag{38}$$

The values of the noise $y_i^{(2)}$ are assumed to be, independently, normally distributed with mean zero and standard deviation σ, a quantity taken to be the *measure of the noise*.

Generally the noise is small compared to the main physical variation, but its effect must be carefully studied since we wish to represent the physical characteristic with as much detail as possible. The noise would produce a very rough and physically unacceptable representation if the original data were fitted exactly without time and space smoothing. Thus a certain amount of smoothing is necessary, but too much smoothing would produce a representation which does not respect well enough the true physical variation of the data. Our problem is therefore to represent as accurately as possible the component $f_1(x)$, given only the sampled values y_i of $f(x)$. We treat first the separation of noise from the diurnal variation.

4.1. Separation of Noise From the Diurnal Variation

We employ a type of mathematical filter [12] which rejects that part of the "signal" (ionospheric data) produced mainly by noise $f_2(x)$ and accepts the part representing mostly true physical variation $f_1(x)$. Our main tool is the Fourier analysis of the sampled values y_i (sec. 3.1) which decomposes the diurnal variation into eleven harmonics

$$c_j \cos (jx-\psi_j)=a_j \cos jx+b_j \sin jx \tag{39}$$

and thereby gives a *discrete power spectrum* c_j. It is shown that some of these harmonics represent mostly $f_1(x)$, whereas the others are produced mainly by $f_2(x)$. The proper separation of these harmonics and resulting truncation of the Fourier series give the optimum smoothing (or filtering) as well as the desired diurnal representation. For determining the proper separation of harmonics [13] we make use of certain properties of the Fourier spectrum which characterize the two component functions of $f(x)$. As a by-product we also obtain a quantitative estimate of the noise σ, which can be compared with results from an independent method.

a. Spectrum for a Real Ionospheric Characteristic $f_1(x)$

It is well known that a smooth, continuous function $f_1(x)$ of period 2π can be expanded in a Fourier series—of functions 1, cos jx and sin jx ($j=1$, 2, 3, . . .)—and that the coefficients, given by integral formulas analogous to (28), approach zero as j increases, at a rate depending upon the smoothness of $f_1(x)$. It can be shown,[14] for example, that if $f_1^{(\prime)}(x)$ is piecewise continuous in $(-\pi,\pi)$ then the coefficients approach zero at least as fast as j^{-1}, whereas if $f^{(\prime\prime)}(x)$ is piecewise continuous the rate is j^{-2}. In general the size of α in the $j^{-\alpha}$ law increases or decreases with the smoothness of $f_1(x)$, so that in a sense the smoothness of a function is characterized by the value of α.

These same laws apply (approximately) to the coefficients a_j and b_j obtained from Fourier analysis of a sample, $y_1^{(1)}$, $y_2^{(1)}$, . . . , $y_{24}^{(1)}$, of hourly values of $f_1(x)$. Thus the squared amplitude $c_j^2=a_j^2+b_j^2$ decreases at least as fast as $j^{-2\alpha}$. When c_j^2 is plotted against j in a log-log scale, the curve defined by smoothing the points on the graph will have a slope less than or equal to -2α. We refer to this value as the *slope of the Fourier spectrum*. It is safe to assume that the real diurnal variation of an ionospheric characteristic has at least a piecewise continuous first derivative. Thus the slope of its spectrum should be -2 or less.

b. Spectrum for a Random Noise Component $f_2(x)$

Let $y_1^{(2)}$, $y_2^{(2)}$, . . ., $y_{24}^{(2)}$ denote a sample of values of the random noise component $f_2(x)$—each value hav-

[12] This type of filter is analogous to a "low-pass electrical filter—i.e., a filter designed to pass only low frequencies while eliminating all frequencies above a certain point [Holloway, 1958]. Such a filtering process is frequently referred to as "smoothing."

[13] The central idea employed is suggested by Lanczos [1956, pp. 331–344].

[14] See [Jackson, 1957, pp. 1–22].

ing an independent normal distribution with mean zero and variance σ^2—and consider a Fourier analysis of these values. The statistical distributions of the Fourier components (a_j, b_j, c_j, and ψ_j) are obtained as a result of the *asymptotic solution for the random walk* [Chapman and Bartels, 1940, pp. 572–582]. Thus it follows from a theorem of Markoff that the coefficients a_j and b_j have independent normal distributions with mean zero and variance $\sigma^2/12$. From this it is shown that the phase ψ_j is *uniformly* distributed in $-180° \leqq \psi_j \leqq 180°$ and that the amplitude c_j has a *Rayleigh* distribution with mean $\sigma\sqrt{\pi/24}$, so that the squared amplitude c_j^2 has the expected value

$$E(c_j^2) = \frac{\sigma^2}{6}. \tag{40}$$

Since these results are independent of the harmonic j, it follows that c_j^2 oscillates about a constant value $\sigma^2/6$, the noise level, and that the Fourier spectrum for random noise has a *slope of zero*.

c. Spectrum for Ionospheric Data

Since the noise is small compared to the main amplitude of the diurnal variation, we would expect—from the theory outlined above—that the spectrum for actual data would decay rapidly for the first

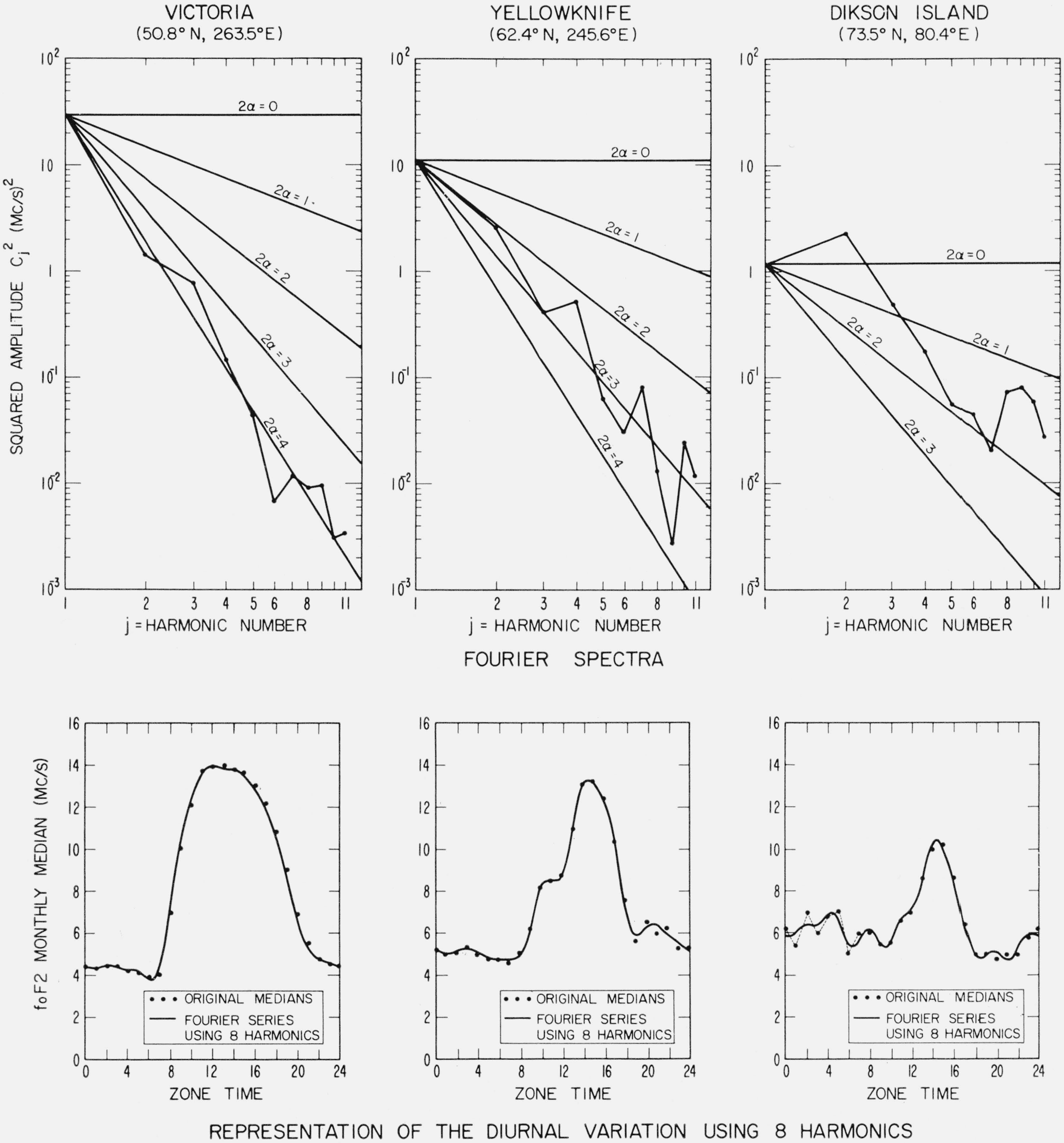

FIGURE 7. *Fourier analysis of the diurnal variation of f_0F_2 monthly medians from three typical stations for December, 1957.*

harmonics and would then level off around a constant value $\sigma^2/6$. The point at which the leveling off takes place separates the harmonics representing mostly true physical variation from those produced mainly by noise. Thus we determine the optimum cutoff for the Fourier series. It is inevitable that a few harmonics will be in a "twilight zone" where the amplitude of the real physical variation is the same as that of the noise. However, it is not of vital importance where the cutoff is made in this region, except that the series should not be extended too far.

To illustrate the method we consider the monthly medians of f_0F_2 from three typical stations (fig. 7). These examples illustrate the relation between smoothness of data and slope of the spectrum. For Victoria, with the smoothest data, the slope of the spectrum (for the lower order harmonics) appears to be -4; for Yellowknife it is around -3; and for Dikson Island it is approximately -2, in beautiful agreement with the theory. In each case the spectra show a tendency to level off around harmonic 7, indicating the effect of noise on the higher harmonics and the position of the twilight zone for the optimum cutoff.

The theory has also been applied to determine the *average optimum cutoff*, using the mean spectrum for all stations for the given month (fig. 8). As was expected the mean spectrum is much smoother than the spectra for the individual stations, so that the slope and optimum cutoff are more clearly defined. There is a definite change in the character of the spectrum at harmonic 8. It is clear that harmonic 7 is above the noise level and so should be retained, but harmonic 8—being in the twilight zone—could either be retained or not. We have terminated the series after the 8th harmonic. The effect of this smoothing process is illustrated for the three stations in figure 7 by the solid lines representing the diurnal variation. It has been found that for other months and other characteristics the mean spectrum is generally as smooth as the one shown in figure 8, but the twilight zone is sometimes more extended.

A number of other studies have been made to determine the average optimum cutoff, in addition to the work on Fourier spectra. From the theory of analysis of random noise, the phase ψ_j for noise harmonics is uniformly distributed; thus all values of the phase are equally likely to occur. By comparing the phase angles from all stations for a given harmonic (by means of polar plots of amplitude and phase), we have found systematic variations with geographic position for the lower harmonics and apparently random (uniform) distributions for higher harmonics, in good agreement with the previous results. Similar investigations have been made to determine the distributions of the other components, a_j, b_j, and c_j. Although reasonably good agreement with the previous studies was found, the results for these cases were not so well defined. This was to be expected, however, since the parameters defining the normal and Rayleigh distributions of these components are subject to geographic variation.

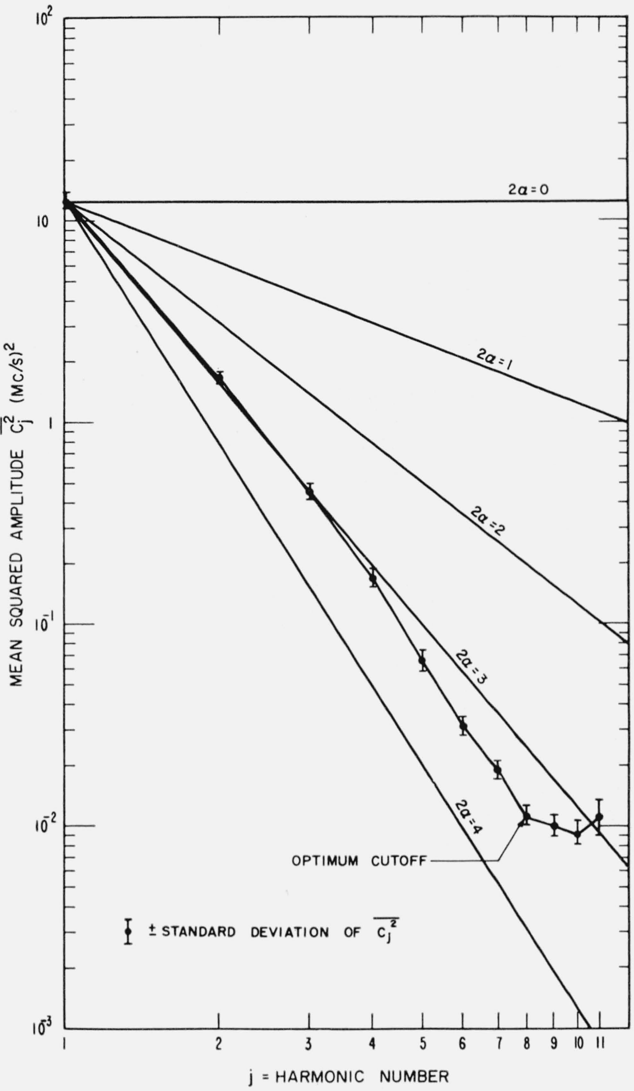

FIGURE 8. *Average Fourier spectrum for* f_0F_2 *monthly medians.*
December 1957 113 stations

d. Estimation of the Noise σ

The theory also provides a means for computing the noise σ. Taking the mean squared amplitude for the noise harmonics

$$\frac{1}{3}\sum_{j=9}^{11} c_j^2$$

as an estimate of $E(c_j^2)$, we use (40) to obtain σ. Values of the noise are given in table 2 for the three sets of data illustrated in figure 7. In a similar manner we compute the *average noise* in f_0F_2 medians for December 1957

$$\bar{\sigma}=\sqrt{6}\left[\frac{1}{3}\sum_{j=9}^{11}\overline{c_j^2}\right]^{1/2}=0.25 \text{ Mc/s}, \qquad (41)$$

where $\overline{c_j^2}$ denotes the mean squared amplitude of the jth harmonic from 113 stations. Calculations of the average noise in f_0F_2 medians made over a period of several years have been found to be closely correlated with solar activity. The details of these studies, however, will be given in a subsequent paper.

TABLE 2. *Noise in* f_0F_2 *medians for December 1957*

Station	Noise σ
	Mc/s
Victoria, B.C	0.18
Yellowknife	.28
Dikson Island	.58

The same estimates of noise have been made by an entirely independent method. Making use of the distributions of daily measurements, we have computed the standard deviations of the sample medians. The good agreement of these independent results gives added strength not only to the estimates of noise, but also to the determination of the optimum smoothing.

Each of the Fourier coefficients is equally affected by noise, but we have shown that for the lower harmonics ($j \leqq 8$) the physical variation is the dominant part, whereas for higher harmonics mostly noise is present. By truncating the Fourier series we have eliminated about 30 percent of the noise—the part contained in the truncated terms—at no loss of real physical variation. A large part of the remaining 70 percent of the noise is filtered in a similar manner by analysis of the geographic variation of the Fourier coefficients. This problem is treated in the following section.

4.2. Separation of Noise From Geographic Variation

The noise is separated from the real geographic variation of Fourier coefficients by a filtering process[15] similar to that used in the preceding section. Having expanded the geographic variation in a series (36) of orthonormal functions $F_k(\lambda,\theta)$ as in section 3.3, we obtain the smoothing (or filtering) by truncating the series. In this case, however, we do not have the elegant theory associated with Fourier analysis for determining the optimum cutoff.

The method employed is based on the *residuals* between the original Fourier coefficients being fitted and the corresponding values of the representation function $Y_K(\lambda,\theta)$ given by (36). Since orthonormal functions were used in the development of $Y_K(\lambda,\theta)$, we can inspect the residuals remaining after each term $d_kF_k(\lambda,\theta)$ is added to the series. The residuals approach zero as the number $K+1$ of terms in the series is increased, and they would actually attain this limit (except for rounding error) when $K+1$ is equal to the number of stations. However, we know that the Fourier coefficients are affected by noise; hence zero residuals are not desired.

The criterion adopted for determining the optimum cutoff is to minimize the standard deviation of the residuals. We take as an *unbiased estimate of the variance of the residuals*

$$e_k^2 = \frac{E_k}{N-k-1} \tag{42}$$

where E_k is the sum of squares of residuals (20), N is the number of stations, and $(N-k-1)$ is the number of degrees of freedom remaining after subtraction of one degree for each term in the series $Y_k(\lambda,\theta)$ [Kendall, 1951, pp. 59–61]. From (42) it is possible for the estimate of the variance e_k^2 (or of the standard deviation e_k) of the residuals to increase as k increases, since the diminishing of E_k may become very slow after a certain degree. For simplicity we shall refer to e_k as the *standard deviation of the residuals*. In the analyses under present consideration, the values e_k usually decrease quite rapidly at first, then taper off and cease to diminish appreciably after a certain point. This point defines the desired optimum cutoff.

In order to determine this cutoff objectively we make use of a statistical test for the significance of each coefficient d_k (in (36)) based on the "Student's" t distribution [Fisher, 1922]. Under the usual assumption that the observed values y_i have independent normal distributions about a mean regression surface with common variance σ^2, it follows that the quantity

$$\frac{d_k - \delta_k}{e_k},$$

where δ_k is the expected value of d_k, has a "Student's" t distribution with $(N-k-1)$ degrees of freedom. Therefore we test the null hypothesis H_0 (i.e., $\delta_k=0$) using a 5 percent rejection criterion

$$\left|\frac{d_k}{e_k}\right| > t_{0.05}.$$

In most of our applications the value of (N−k−1) has been large enough so that $t_{0.05}$ is approximately 2.

Although the test described above is probably the best possible for the present problem, we note here the following limitation. It was assumed that the distributions of all the observed values y_i have a common variance σ^2. It is known, however, that σ^2 varies significantly with geographic location, so that the theory applies only approximately to our problem. As a result the representations are somewhat oversmoothed in certain regions and undersmoothed in others. Since we prefer a slightly undersmoothed representation (in order to represent the physical details as well as possible) we have chosen a 5 percent rejection as opposed to a 1 percent.

As an illustration we consider the determination of the optimum cutoff of the main latitudinal terms (table 1) for representing the Fourier coefficient shown in figure 6. The last term found to be significant was d_{10} and we have therefore terminated the series at this point. A graph of e_k through degree 15 is shown in figure 9 and some of the values e_k and d_k

[15] See the discussion on "smoothing of observational data by the method of least squares" [U.S. Dept. of Commerce, NBS, AMS 9, 1952, pp. 16–18].

are given in table 3. In a similar manner we determine the optimum cutoffs for the first and second order terms in longitude (table 1). In figure 10 is shown the graph of e_k corresponding to the set of coordinate functions $G_k(\lambda, \theta)$ specified by $q_0=10$, $q_1=12$, and $q_2=6$ (sec. 3.3). From our test we find the optimum cutoffs specified by $q_1=7$ and $q_2=5$.

In addition to statistical tests we have also been guided by certain physical properties known to exist in the ionosphere and by some knowledge of the morphology of our mathematical functions. For example, for a polynomial of degree k in $\sin \lambda$ the distance between two adjacent maxima will have to be at least $(360/k)$ degrees. Therefore, in order to represent the sharp dip in critical frequencies known to exist near the magnetic equator (figs. 2 and 3), we know *a priori* that very high degree polynomials are needed.

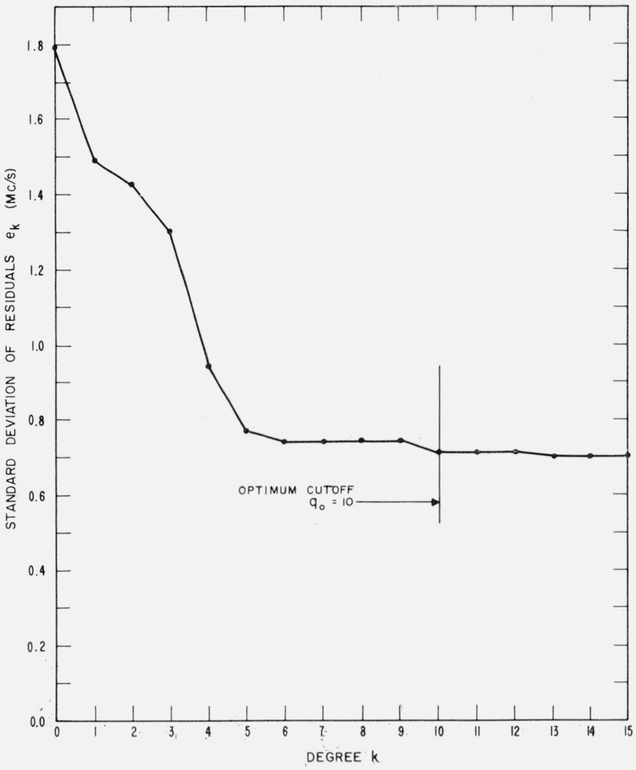

FIGURE 9. *Standard deviation of residuals* e_k *for each degree from the analysis by orthogonal polynomials in* $\sin \lambda$ (λ= *latitude*) *of Fourier (time series) coefficients* a_1 *for* f_0F_2 *monthly medians.*

December 1957 113 stations.

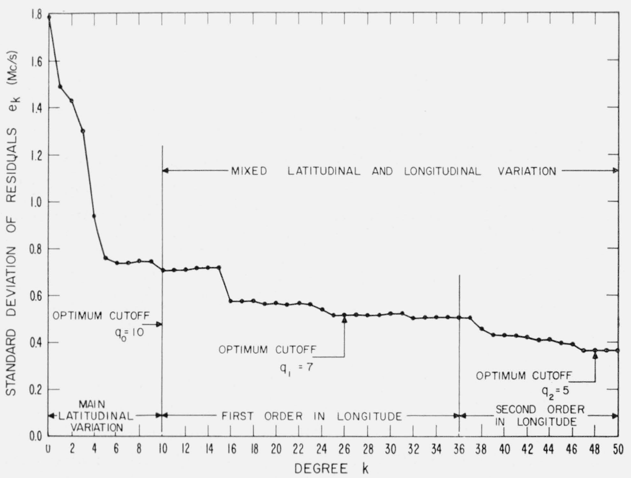

FIGURE 10. *Standard deviation of residuals* e_k *for each degree from the analysis by the geographic functions* G_k (λ, θ) *of Fourier (time series) coefficients* a_1 *for* f_0F_2 *monthly medians.*

December 1957 113 stations.

TABLE 3. *Least squares fitting of spherical harmonic functions* $G_k(\lambda,\theta)$ *to Fourier (time series) coefficients* a_1 *for* f_0F_2 *monthly medians*

December 1957 113 stations.

		k	STANDARD DEVIATION OF RESIDUALS e_k	ORTHONORMAL COEFFICIENTS d_k	COEFFICIENTS FOR FUNCTIONS $G_k(\lambda,\theta)$ D_k
MAIN LATITUDINAL VARIATION		0	0.17912555E 01	0.28253230E 02	0.72834942E 00
		1	0.14878412E 01	0.10660453E 02	0.26530059E 01
		2	0.14296524E 01	-0.45703227E 01	0.21789511E 02
		3	0.12992993E 01	-0.63889114E 01	-0.18330225E 02
		4	0.94112997E 00	-0.93996341E 01	-0.10238298E 03
		5	0.76460836E 00	-0.57535547E 01	0.75444277E 02
		6	0.73723422E 00	-0.22231647E 01	0.24343033E 03
		7	0.73989519E 00	-0.36166392E-00	-0.98828048E 02
		8	0.74338301E 00	-0.97018918E-01	-0.26629260E 03
		9	0.74437083E 00	0.63343991E 00	0.39049190E 02
		10	0.71160986E 00	0.23279645E 01	0.10270473E 03
MIXED LATITUDINAL AND LONGITUDINAL VARIATION	FIRST ORDER IN LONGITUDE	11	0.71333002E 00	0.50874979E 00	0.80027716E 00
		12	0.71428508E 00	-0.61032332E 00	-0.68859721E 00
		13	0.71788294E 00	0.89986758E-02	0.34758507E-00
		14	0.71730649E 00	0.77229120E 00	-0.15318519E-00
		15	0.72056954E 00	0.24375897E-00	-0.11218609E 02
		16	0.57861927E 00	0.42689060E 01	-0.42479381E 01
		17	0.58156729E 00	0.99377523E-01	-0.42751712E 01
		18	0.58294996E 00	-0.43228252E-00	0.98574758E-01
		19	0.57096788E 00	-0.12750213E 01	0.30209412E 02
		20	0.57315171E 00	0.31006010E-00	0.21029317E 02
		21	0.56632543E 00	0.10180058E 01	0.53866997E 01
		22	0.56914243E 00	-0.18124516E-00	0.29883151E-00
		23	0.56555211E 00	-0.82855405E 00	-0.22921705E 02
		24	0.54427645E 00	-0.15484624E 01	-0.16010904E 02
	SECOND ORDER IN LONGITUDE	25	0.54640091E 00	0.30764920E-00	-0.87875202E 00
		26	0.51088715E 00	0.18782187E 01	0.53212479E 00
		27	0.48734745E-00	0.15027802E 01	0.90155041E 00
		28	0.48894281E-00	-0.32661115E-00	-0.75395824E 00
		29	0.46874104E-00	0.13582557E 01	0.18835551E 01
		30	0.46133326E-00	0.88582236E 00	0.19063634E 01

5. Stability of the Geographic Representation

To obtain a "best" representation of the geographic variation, one must consider more than the optimum separation of noise (filtering)—i.e., more than just the residuals at the stations where data are given. The heavy grouping of stations in some regions such as Europe (fig. 1) and the absence of stations in other regions, particularly in the oceans and near the poles, tends to produce a sort of "mathematical instability" in the representation function—that is, unrealistic behavior in the areas where no data are available. This behavior is somewhat analogous to the large fluctuations which arise in Lagrange (polynomial) interpolation of clustered values with small variation [Lanczos, 1956, pp. 346–358].

As we pointed out in chapter 2, the usual approach in the global analysis of geophysical data has been to first draw contour maps by hand (using the actual data, empirical knowledge and experience) and then to analyze in spherical harmonics the values read from the maps at the intersections of a regular grid. Thus the (synthetic) values used in the analysis are uniformly spaced and the mesh of the grid can be made sufficiently small to prevent instabilities in the representation function. This method has the disadvantage of introducing error (noise) both in drawing and in reading the maps. Moreover, the hand work involved is relatively slow and cumbersome. We have eliminated these two difficulties by first analyzing the data *directly* as they are obtained at the ionospheric stations. However, as a result we have had to face still another problem, that of mathematical instability described above.

For a region where there are no available stations, the representation function gives a two-dimensional interpolation determined by the data from all stations, both near the region and far away. Thus the best representation that could be expected is a smooth continuation of the variations from surrounding stations. Strong departures from such smooth continuations are probably artificial and physically meaningless.

Examples [16] of instability can be seen in the contour map (fig. 11a) computed from an analysis using the coordinate functions $G_k(\lambda, \theta)$ (table 1) specified by $q_0=10$, $q_1=7$, $q_2=5$—these were the optimum cutoffs (sec. 4.2) from the viewpoint of separation of noise. Included in the map are the residuals between the original Fourier coefficients and the corresponding values of $Y_{38}(\lambda, \theta)$. Although the fluctuations in this map are not large, there is a definite appearance of *instability in the southern hemisphere*, particularly near the pole. By further truncating the orthonormal series $Y_{38}(\lambda, \theta)$ so as to correspond to the set of $G_k(\lambda, \theta)$ specified by $q_0=10$, $q_1=6$ and $q_2=2$, very little damage is caused in terms of increased residuals. However, as can be verified from the map in figure 11b, considerable advantage is gained in terms of increased stability near the south pole. Table 3 gives the values of e_k and the coefficients d_k and D_k corresponding to these functions.

Thus it is sometimes necessary to make the cutoff slightly above the optimum level (determined by noise) in order to preserve the stability and physical soundness of the representation function. The amount of increase required in the residuals depends upon the world wide coverage of ionospheric stations.

6. Reorthogonalization and the Accumulation of Error

6.1. Accumulation of Error in the Gram-Schmidt Orthogonalization Process

As was pointed out in chapter 2, the normal equations

$$\sum_{k=0}^{K} a_k(A_k,A_m)=(y,A_m) \qquad m=0,1,\ldots,K \tag{43}$$

(analogous to (4)) are *uncoupled* by the condition of orthogonality (6) imposed on the $A_k(x)$. Thus all terms on the left side of (43) vanish except those of the form $a_m(A_m,A_m)$, so that the coefficients a_k are given by (11). Although (11) is *algebraically* exact, it will be shown that the coefficients thus obtained could be strongly affected by accumulative errors of rounding. We let a_k' denote the *theoretically* exact solution to (43) and write for the error in a_k (as computed from (11))

$$\delta a_k=a_k'-a_k=-\sum_{\substack{m=0\\m\neq k}}^{K} a_m'A_{mk} \tag{44}$$

where

$$A_{mk}=\frac{(A_m,A_k)}{(A_k,A_k)}. \tag{45}$$

As an approximation to δa_k we compute

$$\Delta a_k=-\sum_{\substack{m=0\\m\neq k}}^{K} a_mA_{mk}. \tag{46}$$

Thus if some of the numbers A_{mk}, $m\neq k$, differ significantly from zero (i.e., have nonzero digits among those retained by the computer), it is likely that large values of Δa_k will occur. When we look closely at the orthogonalization process (sec. 2.2), it is not too surprising to find that some of the A_{mk} are significantly different from zero, particularly if the coordinate functions $G_k(x)$ are not approximately orthogonal. This can be seen as follows.

The functions $A_k(x)$ are constructed successively according to (8) and (9). In fact, multiplying (8) by $A_m(x)$, $m<k$, and summing over the x_i gives

$$(A_k,A_m)=\sum_{p=0}^{k-1} a_{kp}(A_p,A_m)+(G_k,A_m). \tag{47}$$

Then imposing the orthogonality condition (6) on the left member above, we have

$$a_{km}=-\frac{(G_k,A_m)}{(A_m,A_m)}-\sum_{\substack{p=0\\p\neq m}}^{k-1} a_{kp}A_{pm}, \tag{48}$$

and (9) follows by neglecting the terms $-a_{kp}A_{pm}$, $(p\neq m)$ which are (theoretically) zero. From (48) we obtain as an estimate of the *relative* error in a_{km}

$$\frac{\Delta a_{km}}{a_{km}}=-\sum_{\substack{p=0\\p\neq m}}^{k-1} a_{kp}\frac{A_{pm}}{a_{km}}=-\sum_{\substack{p=0\\p\neq m}}^{k-1}(G_k,F_p)\frac{(F_p,F_m)}{(G_k,F_m)} \tag{49}$$

making use of (9), (21), (23), and (45). At this point it is convenient to consider the functions $G_k(x)$, $A_k(x)$, and $F_k(x)$ as N dimensional vectors whose components are the functional values at the points $x_1, x_2, \ldots, x_N$. Then a number such as (G_k,F_p) can be interpreted as the component of the vector G_k in the direction of F_p. For the present we shall consider a typical term on the far right side of (49);

[16] Other examples in one dimension are illustrated in the behavior near the poles of the polynomials in λ (figs. 2 and 3.)

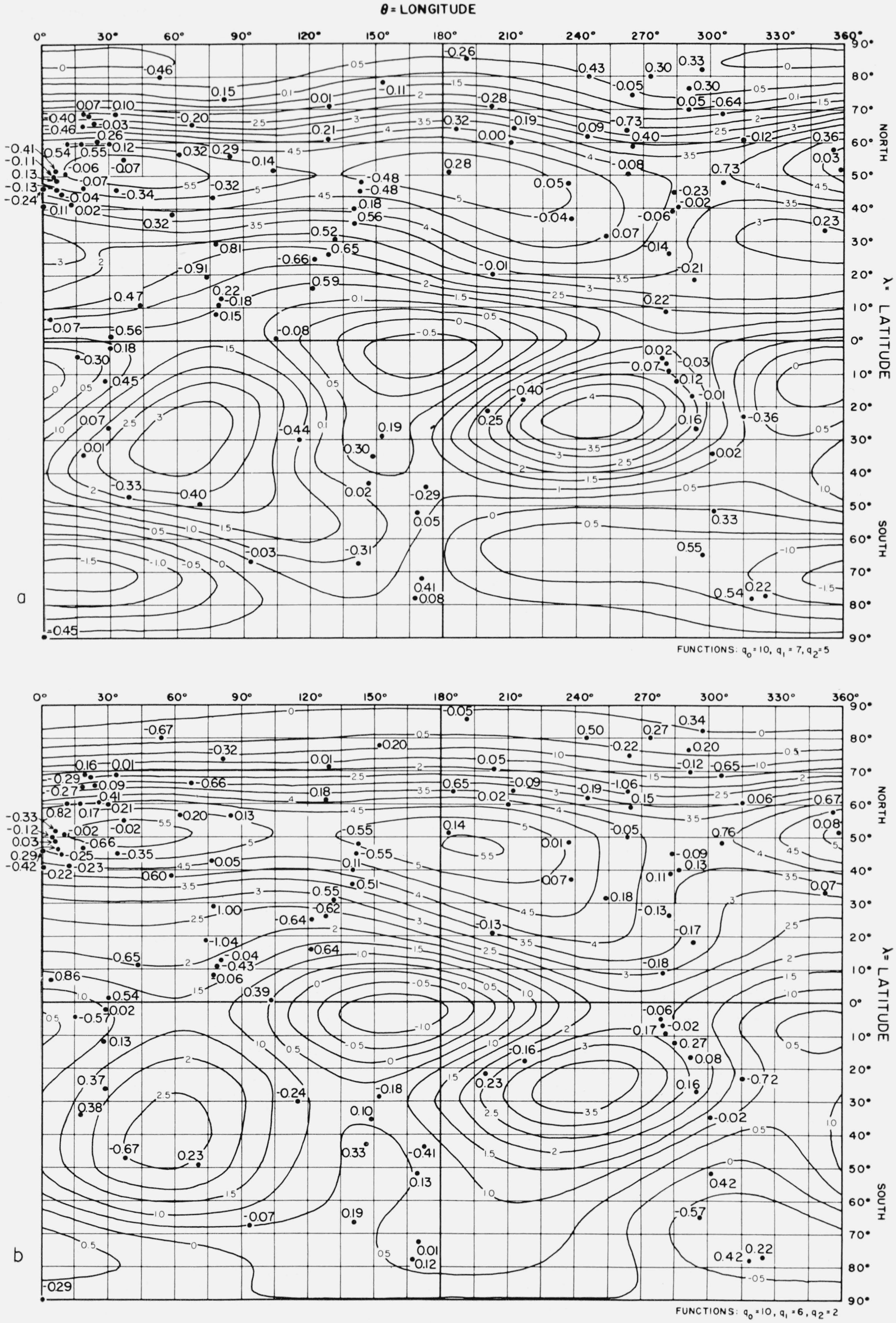

FIGURE 11. *Maps of Fourier (time series) coefficient* a_1 (Mc/s) *and residuals from analyses made with geographic functions* G_k (λ, θ) *for* f_0F_2 *medians.*

December 1957 113 stations.

thus we can assume, without loss of generality, that the G_k are normalized in the sense of (17). Suppose now that G_k has a large component in the direction of F_p (say $(G_k,F_p)=\frac{1}{2}$) but a very small component in the direction of F_m, so that (G_k,F_m) is of the same order of magnitude as (F_p,F_p). Then the resulting error in a_{km} could be as large as 50 percent.

It is clear from the preceding discussion how significant errors can be introduced, the most important factor being the direction of each G_k relative to the preceding F_p, $p<k$. Although such an error may be small, its effect accumulates rapidly since each subsequent $A_k(x)$ is constructed in terms of all preceding $A_m(x)$, $m<k$. Thus a small initial error in one $A_k(x)$ can have disastrous effects on the later steps of the process.

As an illustration we consider the geographic representation of the Fourier coefficient, used in section 4.2, expanded in terms of the coordinate functions $G_k(\lambda,\theta)$ specified by $q_0=10$, $q_1=6$, $q_2=2$ (see table 1). The least squares coefficients a_k computed from (11) and the estimates of the relative error $(\Delta a_k/a_k)$ from (46) are given in table 4. As can be seen the precision of the a_k for $k>7$ is very doubtful. It is shown in the following section that a_8 is off by 5 percent, and other coefficients by considerably more, thus illustrating the usefulness of error estimates.

6.2. Gram-Schmidt Reorthogonalization

In section 6.1 we arrived at the following three important results: (1) large errors can be produced by the process of Gram-Schmidt orthogonalization, (2) eq (46) gives an effective method for estimating such errors, and (3) once started, an error has a strong accumulative effect, but its main source initially is closely related to the "directions" of the coordinate functions $G_k(x)$. If the $G_k(x)$ are nearly *linearly dependent*, the error would develop quickly, whereas if they are approximately orthogonal, the source of error would be greatly reduced. Upon this fact we justify a *Gram-Schmidt reorthogonalization*[17] process, following the same lines as section 2.2, but taking as coordinate functions the $A_k(x)$ instead of the $G_k(x)$. For, although the $A_k(x)$ may not be sufficiently orthogonal for our purpose, they would in general be considerably more so than the original coordinate functions. Thus the initial source of the error would be reduced. The reorthogonalization process can, of course, be repeated as many times as necessary to keep the error under control. Before giving a numerical example, we outline briefly the steps involved in the process.

Following the procedure of section 2.2, we form a new set of orthogonal functions

[17] The notion of *reorthogonalization* was suggested by the Numerical Analysis Section (11.01) of the National Bureau of Standards.

TABLE 4. *Elimination of accumulative rounding error by reorthogonalization process used to fit spherical harmonic functions of latitude and longitude to Fourier (time series) coefficients* a_1 *for* f_0F_2 *monthly medians*

December 1957 113 stations.

	ORTHOGONAL COEFFICIENTS		DEVIATION OF a_k IN PERCENT	ESTIMATES OF ACCUMULATIVE ROUNDING ERROR FROM:	
	FIRST ORTHOGONALIZATION	SECOND ORTHOGONALIZATION		FIRST ORTHOGONALIZATION	SECOND ORTHOGONALIZATION
k	a_k	b_k	$\frac{b_k-a_k}{b_k}$	$\frac{\Delta a_k}{a_k}$	$\frac{\Delta b_k}{b_k}$
0	2.6578404E 00	2.6578404E 00	0.	2.9041629E-06	0.
1	1.5929625E 00	1.5929624E 00	-0.0000063	2.6005150E-06	0.
2	-1.4231348E 00	-1.4231393E 00	0.00032	1.9663900E-05	5.2353136E-08
3	-3.8013159E 00	-3.8013174E 00	0.000040	-4.8294410E-06	3.9199992E-08
4	-1.1098262E 01	-1.1098265E 01	0.000027	7.0032999E-05	0.
5	-1.4189972E 01	-1.4190128E 01	0.0011	-1.1172427E-04	8.4008608E-09
6	-1.0993559E 01	-1.0990924E 01	-0.024	5.3348242E-03	1.0846157E-08
7	-3.5136985E 00	-3.5109766E 00	-0.078	-2.8899443E-02	-2.5464985E-07
8	-1.7760643E 00	-1.8776263E 00	5.4	1.1386564E 00	6.2695740E-07
9	2.3313985E 01	2.3232524E 01	-0.35	1.2002318E-02	4.1049105E-08
10	1.7978380E 02	1.8443359E 02	2.5	1.6151702E-02	0.
11	1.0436464E-01	1.1301300E-01	7.7	3.0752875E-02	0.
12	-1.2964101E-01	-1.2419979E-01	-4.4	-3.1891573E-02	7.4985841E-09
13	3.1378034E-03	3.4149244E-03	8.1	3.2888361E-01	7.6702861E-07
14	3.5222762E-01	3.3267845E-01	-5.9	-3.2077405E-02	1.1197871E-07
15	2.7970650E-01	2.4467795E-01	-14.	-3.0703257E-02	-2.0554128E-07
16	3.6830783E 00	3.6748188E 00	-0.22	-5.6580728E-03	0.
17	2.3149930E-01	1.7777535E-01	-30.	-1.3896600E-01	3.9814584E-07
18	-7.6929165E-01	-7.4671454E-01	-3.0	-5.5304769E-02	-1.4966725E-07
19	-4.8753538E 00	-4.7861179E 00	-1.9	-3.4774151E-02	3.7360954E-08
20	1.1794396E 00	1.0771025E 00	-9.5	-1.6933961E-01	-1.3834487E-07
21	7.3562072E 00	7.2621238E 00	-1.3	-3.2170044E-03	-3.2830421E-08
22	-1.5848168E 00	-1.3387020E 00	-18.	-9.4834993E-02	-7.7917363E-08
23	-1.2521099E 01	-1.2175401E 01	-2.8	4.4063769E-03	4.8954975E-08
24	-2.3682257E 01	-2.3369081E 01	-1.3	-3.2909461E-02	-1.0202309E-08
25	8.9367033E-02	9.1821058E-02	2.7	-6.0492957E-03	-6.0856796E-08
26	5.9681830E-01	5.9769819E-01	0.15	1.3858429E-03	0.
27	1.0897222E 00	1.1006036E 00	0.99	1.1943727E-02	0.
28	-2.7559001E-01	-2.7433266E-01	-0.46	6.7750021E-03	-2.7158927 -08
29	2.2791040E 00	2.2946516E 00	0.68	6.1824901E-03	2.5975466 -08
30	1.9115768E 00	1.9063635E 00	-0.27	1.0157171E-04	4.6899223 -08

$$B_0(x)=A_0(x) \tag{50}$$

$$B_k(x)=\sum_{p=0}^{k-1} b_{kp}B_p(x)+A_k(x),$$

where

$$b_{kp}=-\frac{(A_k, B_p)}{(B_p, B_p)} \tag{51}$$

Then the least squares solution can be written in the form

$$Y_K(x)=\sum_{k=0}^{K} b_k B_k(x) \tag{52}$$

where

$$b_k=\frac{(y, B_k)}{(B_k, B_k)}. \tag{53}$$

To obtain $Y_K(x)$ in the simpler form (1), we compute first the coefficients a_k^* for expressing (52) in terms of the $A_k(x)$. This is done by means of (13) and (14) with a_k, a_{kp}, and D_k replaced by b_k, b_{kp}, and a_k^*, respectively. Then the desired coefficients D_k are obtained using (13) and (14) with a_k replaced by a_k^*. The normalization of the solution is made by means of a similar modification of section 2.3.

For illustration we continue with the same example given at the end of section 6.1. The coefficients b_k and estimates of the relative error $(\Delta b_k/b_k)$ from one reorthogonalization are given in table 4. From these results it is seen that the largest value of the relative error is of the order of 10^{-7}. Thus a great improvement has been gained. Using the coefficients b_k we have computed the relative deviation of the a_k in percent, from which it can be seen that a_{17} differs by as much as 30 percent. Moreover, the breakdown of the first orthogonalization at $k=8$ is clearly shown.

7. Summary of Analysis and Numerical Maps

We summarize here the steps used in the analysis described in the preceding sections (see table 5). The analysis begins with the actual observations as they are tabulated at the stations, each in its own zone time. The *diurnal* representation is obtained from Fourier analysis of the 24 hourly values (for each station), the corrections to LMT being produced by an appropriate shift of the phase, determined by the station locations. The optimum separation of the noise from the real physical variation of the data is made by truncating the high frequency harmonics (low-pass filtering). Thus for the characteristic f_0F_2, only 8 harmonics are needed. The *geographic* variation of each of the 17 Fourier coefficients

$$a_0 b_1 a_1 b_2 a_2 \ . \ . \ . \ b_8 a_8 \tag{54}$$

is represented by an orthonormal series, analogous to spherical harmonic analysis. Since the functions in these series must be orthogonal relative to the coordinates (λ_i, θ_i) of the stations, they cannot be known *a priori;* hence they must be constructed. Gram-Schmidt orthogonalization and reorthogonalization are used for this purpose. The smoothing (filtering) in the geographic dimensions is then performed by truncating the orthonormal series for each of the 17 Fourier coefficients.

The end product of the analysis is a table of numerical coefficients D_{sk} defining a function $\Gamma(\lambda,\theta,t)$ of the form

$$\Gamma(\lambda,\theta,t)=a_0(\lambda,\theta)+\sum_{j=1}^{H}[a_j(\lambda,\theta)\cos jt+b_j(\lambda,\theta)\sin jt] \tag{55}$$

where each of the functions $a_j(\lambda,\theta)$ and $b_j(\lambda,\theta)$—representing the geographic variations of the Fourier coefficients—is a series of the form

$$\sum_{k=0}^{K} D_{sk}G_k(\lambda,\theta) \tag{56}$$

(see table 1). The index s denotes which Fourier coefficient is represented in the order shown in (54).

TABLE 5. *Summary diagram of the analysis*

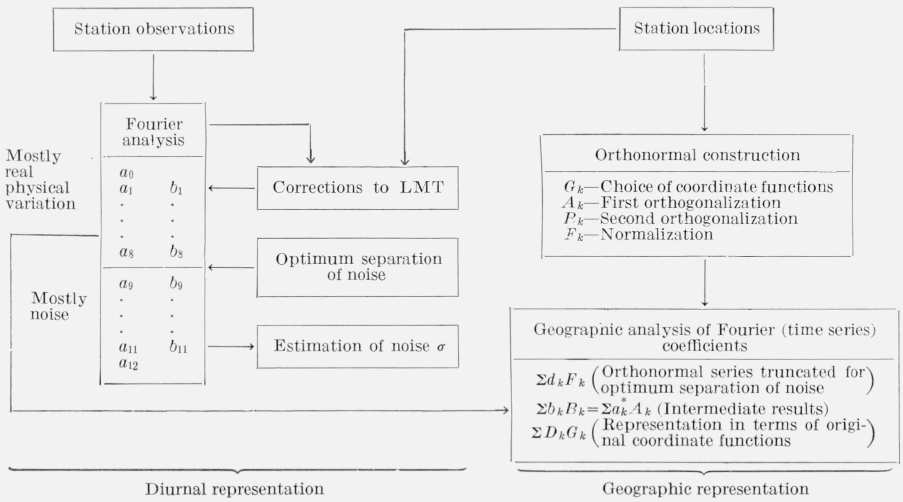

TABLE 6. *Coefficients D_{sk} defining the function Γ (λ, θ, t) for monthly median f_0F_2 (Mc/s), December 1957*

I—main latitudinal variation. Mixed latitudinal variation: II—first order in longitude, III—second order in longitude. Notation: For each entry the number given by the first eight digits and sign is multiplied by the power of 10 defined by the last two digits and sign.

TIME VARIATION

GEOGRAPHICAL VARIATION

Harmonic		0	1		2		3		4	
	K \ S	0	1	2	3	4	5	6	7	8
I	0	1.0914267E 01	7.7372089E-01	7.283[illegible]942E-01	-9.2623643E-01	8.7422963E-01	-1.7848102E-01	-3.7885388E-01	2.9685747E-01	-2.5333249E-01
	1	-7.8953766E-01	4.8827410E-01	2.6530059E 00	-1.5247263E 00	8.0915360E-01	-9.4284316E-01	-1.7684497E 00	-4.3241333E-01	-5.7663186E-01
	2	2.9886163E 00	1.6714562E 01	2.1789511E 01	6.5370734E-01	-3.3546872E 00	-2.3955230E-01	-1.4676821E 00	-1.4250625E 00	-4.1630597E-01
	3	1.5785872E 01	1.7292880E 00	-1.8330226E 01	3.4795284E 00	-4.3719376E 00	6.4229818E 00	1.0586009E 01	9.2466606E 00	2.8930649E-02
	4	-7.3081383E 01	-1.0531759E 02	-1.0238298E 02	2.1601855E 00	8.6228765E 00	-6.8914741E-01	1.0163215E 01	1.0430091E 01	6.1317524E 00
	5	-4.6525828E 01	-4.1977129E 00	7.5444276E 01	2.0150497E 00	1.6324815E 01	-3.4641695E 01	-2.6678432E 01	-3.7404618E 01	-5.6494755E-01
	6	1.9878676E 02	2.5449798E 02	2.4343033E 02	-4.3352216E 00	-5.4578438E 00	-7.5223076E 00	-2.2052303E 01	-3.9342693E 01	-2.0193537E 01
	7	4.9107151E 01	8.4645829E 00	-9.8828049E 01	-2.6254765E 00	-1.7752290E 01	6.0494795E 01	3.1563795E 01	5.0754311E 01	4.2224289E 00
	8	-2.1057577E 02	-2.6631189E 02	-2.6629260E 02	1.1159760E 01	-1.8912893E-01	2.3693942E 01	2.5115734E 01	5.3091602E 01	2.7875168E 01
	9	-1.7550868E 01	-6.6770028E 00	3.9049190E 01	-1.4319514E 00	5.0474002E 00	-3.1529647E 01	-1.3718612E 01	-2.2160749E 01	-3.1592644E 00
	10	7.6640091E 01	1.0001173E 02	1.0270474E 02	-8.8129838E 00	-5.9311831E-01	-1.5101959E 01	-1.1473124E 01	-2.3054411E 01	-1.3278131E 01
II	11	-5.2964947E-01	2.4364768E-03	8.0027715E-01	6.0721534E-01	-1.2101191E-01	-1.0403821E-01	1.6257809E-01	-1.0643796E-01	6.2557100E-02
	12	2.6902534E-01	9.4759300E-02	-6.8859721E-01	7.3459486E-01	1.7502589E-01	-5.0371087E-02	3.1257521E-01	-7.8402439E-02	6.3306112E-02
	13	2.1349603E-02	-3.9538481E 00	3.4758507E-01	3.0601999E 00	-1.2871614E-01	-4.8954588E-02	9.1777242E-01	-4.7842801E-01	-1.8609319E-02
	14	3.1711371E 00	1.7516087E 00	-1.5318519E-01	1.2964863E 00	7.3990802E-01	-8.4662998E-01	2.2758654E-01	-2.2977208E-02	-1.0258091E-01
	15	1.6633779E 00	-3.5908690E 00	-1.1218609E 01	-5.7828038E 00	-5.0241930E-01	7.0223299E-01	-1.4589699E 00	1.1074558E 00	-5.0288115E-01
	16	-5.3166566E 00	-5.6115813E 00	-4.2479382E 00	-7.8961277E 00	7.7927373E-02	2.7583131E 00	-1.7414663E 00	7.5675662E-01	-8.2908363E-01
	17	-1.9191693E-01	1.6253567E 01	-4.2751713E 00	-1.0306968E 01	4.1552535E-01	7.0501295E-01	-4.5479047E 00	8.5073202E-01	-2.4932280E-01
	18	-2.2335084E 00	-6.0404139E 00	9.8574758E-02	-6.3966695E 00	-1.4409493E 00	3.3823205E 00	-1.9706686E 00	1.9771550E-02	-6.9674328E-03
	19	2.1297312E-01	8.3133165E 00	3.0209412E 01	1.2918815E 01	2.0064190E 00	-1.4150307E 00	1.6666640E 00	-1.5010523E 00	8.8937262E-01
	20	4.1376244E 00	2.0858187E 01	2.1029316E 01	1.8395100E 01	-4.3110338E 00	-1.2203444E 01	2.3400389E 00	-1.0840088E 00	1.2606628E 00
	21		-1.3460412E 01	5.3866998E 00	7.1701701E 00	-8.9934726E-02	-1.3007687E 00	4.4833956E 00		
	22		3.7958689E 00	2.9883151E-01	6.3709797E 00	9.0028155E-01	-3.2107806E 00	1.9325332E 00		
	23		-6.2877868E 00	-2.2921706E 01	-8.3322061E 00	-2.3156345E-01	1.1989445E 00	6.0279800E-01		
	24		-1.6428649E 01	-1.6010904E 01	-1.1403061E 01	4.9586704E 00	1.1153906E 01	-6.5103689E-01		
III	25		4.6818604E-01	-8.7875202E-01	-1.8927348E-02	2.8565115E-01	8.5442873E-02	-3.1833852E-02		
	26		-1.4529204E-01	5.3212479E-01	1.5694889E-01	-1.0888240E-01	1.7714674E-03	1.4413557E-02		
	27		-9.6026849E-02	9.0155041E-01	2.4230455E-01	-5.1621379E-02				
	28		-2.7047523E-01	-7.5395824E-01	4.0790479E-01	8.3877255E-02				
	29		-1.4390941E 00	1.8835552E 00						
	30		1.3630296E 00	1.9063635E 00						

GEOGRAPHICAL VARIATION

Harmonic		5		6		7		8	
	K \ S	9	10	11	12	13	14	15	16
I	0	1.5531158E-01	2.3792567E-01	-6.4560618E-02	6.1802934E-02	-7.2905440E-02	-6.1891910E-02	7.4823447E-02	-1.3109944E-03
	1	3.7190015E-01	-4.9630663E-01	3.7675107E-01	3.1683339E-01	-1.4461850E-01	2.4323151E-01	-1.0825114E-01	-1.0503997E-01
	2	1.0722732E-01	-6.4481278E-01	1.4638798E 00	-5.7878543E-01	-3.7733971E-01	-3.0163709E-01	-5.3879264E-01	-9.2140743E-03
	3	-2.7126487E-01	7.9842262E 00	-1.8491821E 00	1.1859947E-01	-1.4023915E 00	-2.1925556E 00	7.0639567E-01	-3.1251254E-01
	4	-2.0074097E 00	-9.5196921E-01	-1.0122759E 01	6.0368895E 00	3.5854293E 00	4.5672736E 00	1.4057245E 00	-1.6983739E 00
	5	3.0534070E-01	-3.1520131E 01	3.9806334E 00	-2.7641763E 00	7.4862415E 00	7.7719395E 00	-2.5793256E 00	1.9127105E 00
	6	6.2490299E 00	1.6007400E-01	2.9222164E 01	-1.9459016E 01	-8.4682503E 00	-1.1667597E 01	-3.4862643E 00	7.5111334E 00
	7	-2.5598377E 00	4.3334295E 01	-3.4801114E 00	3.3851973E 00	-1.0514823E 01	-1.0894292E 01	3.9185429E 00	-2.6382915E 00
	8	-8.5661732E 00	4.7626390E 00	-3.4945636E 01	2.3111368E 01	7.8529029E 00	1.1465121E 01	5.0508122E 00	-1.0165159E 01
	9	2.1710776E 00	-1.9401572E 01	9.0533099E-01	-1.0657850E 00	4.6367167E 00	5.1017995E 00	-1.9346376E 00	1.1577847E 00
	10	4.0764945E 00	-3.6110235E 00	1.4435670E 01	-9.1508738E 00	-2.4935791E 00	-4.0293859E 00	-2.4991334E 00	4.3718649E 00
II	11	5.2536049E-03	4.5441154E-03	2.7549960E-02	4.8208075E-02	9.6875999E-04	-8.5190815E-03	-5.1576599E-03	-8.1442986E-04
	12	-5.3775538E-02	-3.1418646E-02	6.6945602E-02	2.2478048E-02	-2.8802577E-02	1.0904388E-02	-2.6393688E-02	1.2157885E-02
	13	7.1804160E-02	5.2992250E-02	2.2264430E-02	2.7159531E-02	1.7879777E-03	3.3803478E-03	-4.6019688E-03	-2.2794990E-02
	14	6.1635942E-02	-3.0900826E-02	-8.3197396E-02	5.4742761E-02	3.2164980E-02	-1.8425275E-03	4.8023952E-02	1.0659245E-03
	15	-1.1925527E-02	-5.1757125E-02	-5.0750350E-02	-7.1205906E-02				
	16	1.0552388E-01	4.9768387E-02	-1.1215977E-01	-6.3709289E-02				

The function $\Gamma(\lambda,\theta,t)$ therefore represents the continuous time variations of an ionospheric characteristic on a worldwide basis and can be used to compute its value at any desired location and instant of time. Such a function is referred to as a *numerical map*. The coefficients defining the numerical map of f_0F_2 median for December 1957 are given in table 6.

Many useful applications are made from numerical maps. For example, a variety of worldwide contour maps and other graphical representations of ionospheric characteristics can be computed and plotted automatically by machine. As an illustration, figures 12 and 13 show the variation of f_0F_2 median for fixed instants of universal time (UT) and LMT, respectively. In addition, a great deal can be and has been learned about the regularities of the ionosphere from numerical representations. The most important immediate application, however, is the prediction of long-term changes in ionospheric conditions. Such predictions have already been produced using the methods described here. A further discussion of these results and other applications of numerical mapping will be given in later papers.

The authors give special acknowledgment to the valuable assistance of Mrs. G. Anne Hessing and Miss Martha Hinds in the development and large-scale application of computer programs and to Mrs. J. Kaye Myers for her contributions—particularly in the preparation of ionospheric data on punched cards—essential for the success of the project. The authors also acknowledge the helpful assistance given to them by the operators in the Computing Laboratories of the National Bureau of Standards (in Boulder, Colo., and in Washington, D.C.), Mr. Walter B. Chadwick (Prediction Services) and the Ionosphere World Data Center for supplying the raw ionospheric data employed, and the many other persons at the Central Radio Propagation Laboratory—too numerous to mention—who have rendered useful contributions to this work. Finally, the authors express their sincere appreciation to Dr. Ralph J. Slutz who, as Chief of the Radio Propagation Physics Division and later as consultant for the Upper Atmosphere and Space Physics Division, gave strong support and unceasing encouragement during the entire course of the work.

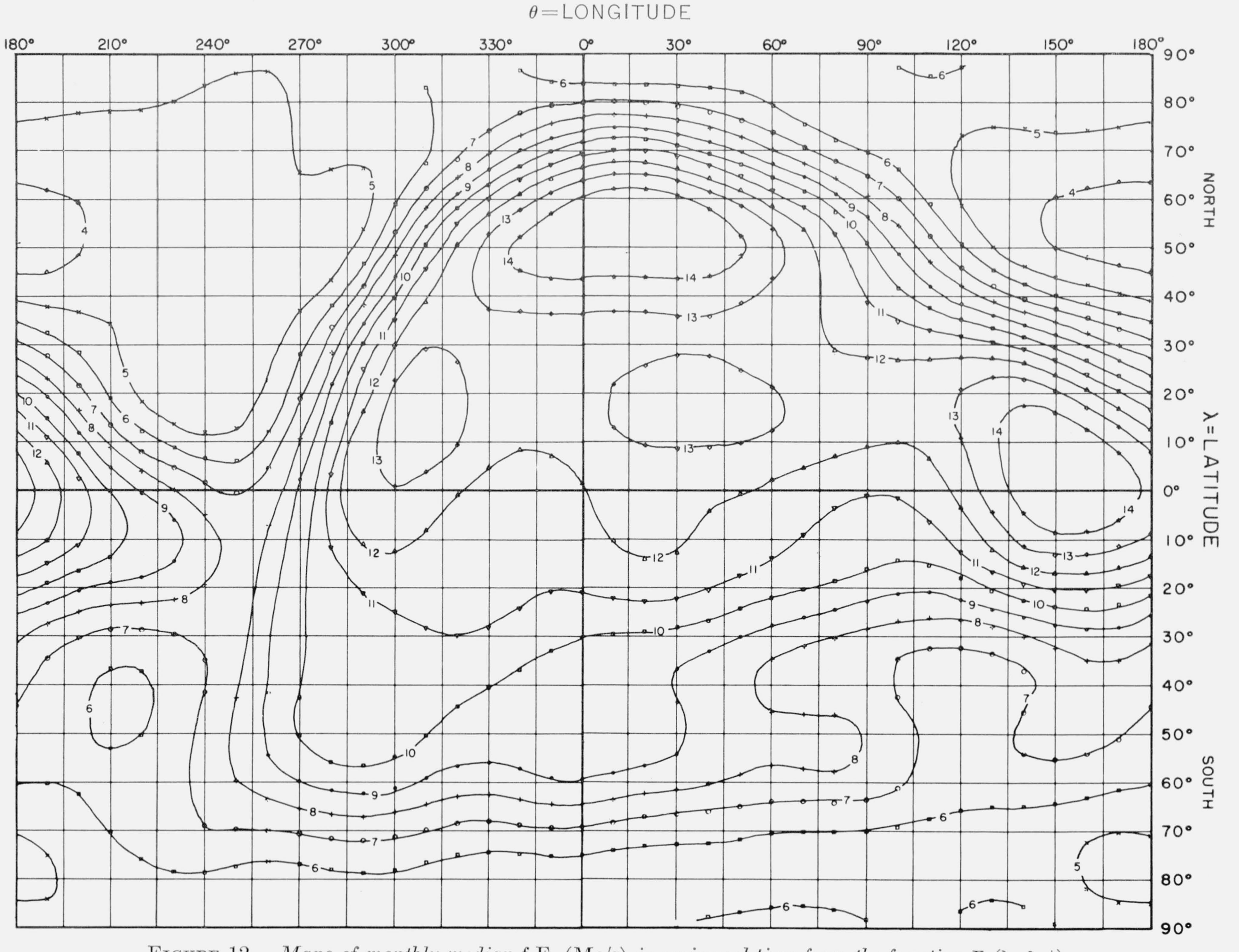

FIGURE 12. *Maps of monthly median* f_0F_2 (Mc/s) *in universal time from the function* Γ (λ, θ, t).

December 1957 UT=12h.

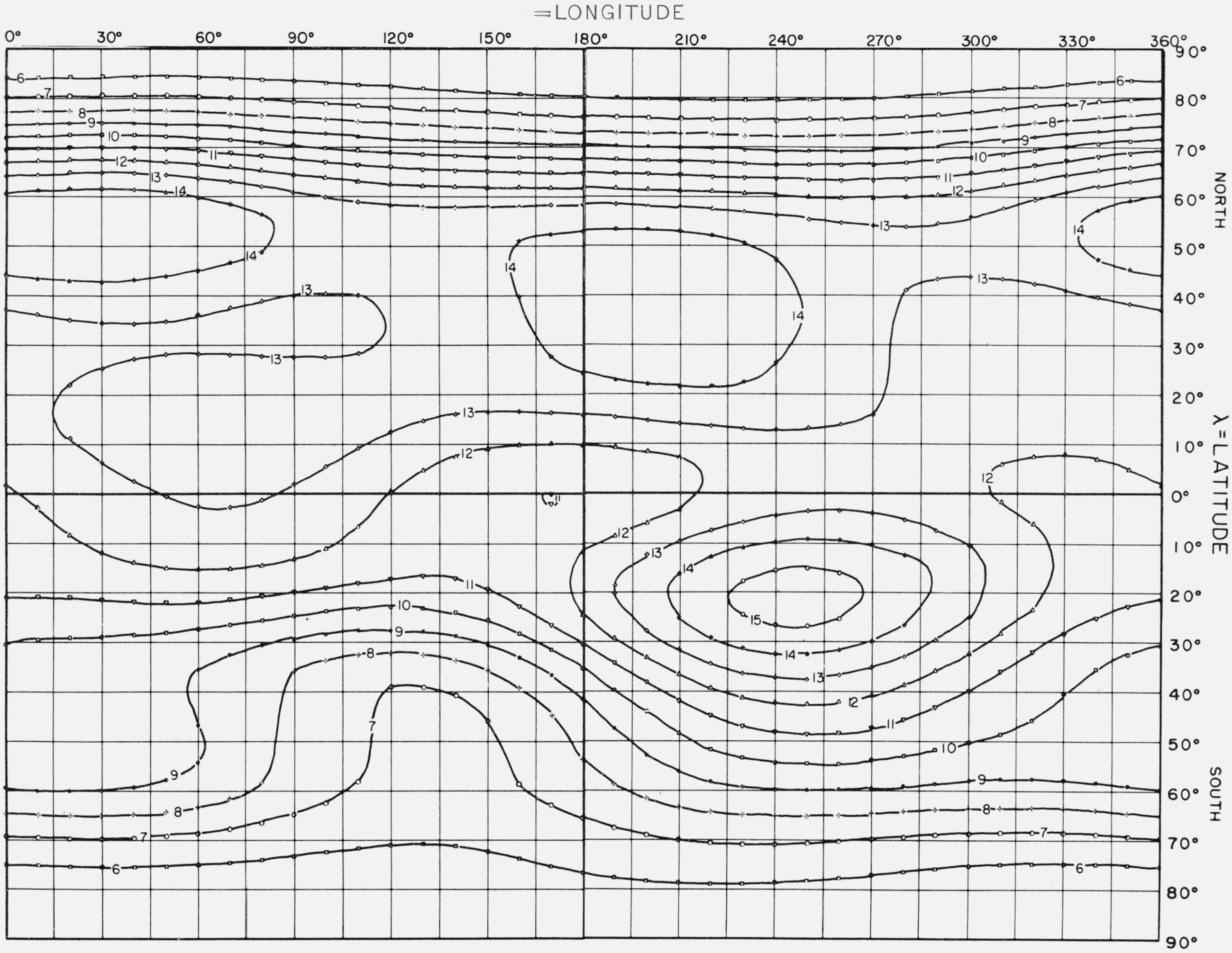

FIGURE 13. *Maps of monthly median* f_0F_2 (Mc/s) *in local mean time from the function* Γ (λ, θ, t).
December 1957 LMT=12h.

8. References

Byerly, W. E., Fourier series and spherical, cylindrical, and ellipsoidal harmonics (Ginn and Company, Boston, 1893).

Chapman, S. and J. Bartels, Geomagnetism, vol. II (Oxford at the Clarendon Press, 1940).

C.C.I.R. Report No. 162 and Study Programme No. 149, Documents of the Plenary Assembly, Los Angeles (1959) (Published by the International Telecommunication Union, Geneva).

Davis, P. and P. Rabinowitz, A multiple purpose orthonormalizing code and its uses, J. Assoc. for Computing Machinery **1,** 183–191 (Oct. 1954).

Fisher, R. A., The goodness of fit of regression formulae and the distribution of regression coefficients, J. of the Royal Statistical Society vol. **LXXXV,** pt. IV, 597–612 (1922).

Forsythe, G. E., Generation and use of orthogonal polynomials for data-fitting with a digital computer, J. Soc. Indust. Appl. Math. **5,** No. 2, 74–88 (June 1957).

Forsythe, G. E. and P. C. Rosenbloom, Surveys in applied mathematics V, Numerical analysis and partial differential equations (John Wiley & Sons, Inc., New York, N.Y., 1958).

Holloway, J. L., Jr., Smoothing and filtering of time series and space fields, from Advances in geophysics, edited by H. E. Landsberg and J. Van Mieghem, **4,** (Academic Press, Inc., New York, N.Y., 1958).

Jackson, D., Fourier series and orthogonal polynomials (The Mathematical Association of America, Carus Mathematical Monograph, No. 6, Buffalo, N.Y., 1941).

Jones, W. B., Atlas of Fourier coefficients of diurnal variation of foF2, NBS Tech. Note 142 (PB161643) (April 1962).

Jones, W. B. and R. M. Gallet, Ionospheric mapping by numerical methods, J. of the International Telecommunication Union, No. 12 (Dec. 1960).

Jones, W. W., J. C. P. Miller, J. F. C. Conn, and R. C. Pankhurst, Tables of Chebychev polynomials, **62** (Roy. Soc. Edin. Proc., 187–203, 1946).

Kendall, M. G., The advanced theory of statistics, vol. **II** (Hafner Publishing Co., New York, N.Y., 1951).

Kunz, K. S., Numerical analysis (McGraw-Hill Book Co., Inc., New York, N.Y., 1957).

Lanczos, C., Trigonometric interpolation of empirical and analytic functions, J. Math. Phys., **17,** 123–199 (1938).

Lanczos, C., Applied analysis (Prentice Hall, Inc., Englewood Cliffs, N.J., 1956).

Stiefel, E. L., On numerical methods of Tchebycheff approximation, from On numerical approximation, edited by R. E. Langer, 217–232 (University of Wisconsin Press, 1959).

Szegö, G., Orthogonal polynomials (American Mathematical Society, Colloquium Publications, vol. **23,** New York, N.Y. 1959).

U.S. Dept. of Commerce, National Bureau of Standards, A.M.S. 9, Tables of Chebychev polynomials $S_n(x)$ and $C_n(x)$ (U.S. Gov't Printing Office, Washington 25, D.C., 1952).

(Paper 66D4–205)